Structure and Function of Viral Deubiquitinating Enzymes

Bailey-Elkin, B.A.; Knaap, R.C.M.; Kikkert, M.; Mark, B.L.

Since January 2020 Elsevier has created a COVID-19 resource centre with free information in English and Mandarin on the novel coronavirus COVID-19. The COVID-19 resource centre is hosted on Elsevier Connect, the company's public news and information website.

Review

Structure and Function of Viral Deubiquitinating Enzymes

Ben A. Bailey-Elkin [1], Robert C.M. Knaap [2], Marjolein Kikkert [2] and Brian L. Mark [1]

*1 - **Department of Microbiology,** University of Manitoba, Winnipeg, Manitoba R3T2N2, Canada*
*2 - **Department of Medical Microbiology,** Leiden University Medical Center, 2333 ZA Leiden, The Netherlands*

***Correspondence to Brian L. Mark:** brian.mark@umanitoba.ca*
http://dx.doi.org/10.1016/j.jmb.2017.06.010

Abstract

Post-translational modification of cellular proteins by ubiquitin regulates numerous cellular processes, including innate and adaptive immune responses. Ubiquitin-mediated control over these processes can be reversed by cellular deubiquitinating enzymes (DUBs), which remove ubiquitin from cellular targets and depolymerize polyubiquitin chains. The importance of protein ubiquitination to host immunity has been underscored by the discovery of viruses that encode proteases with deubiquitinating activity, many of which have been demonstrated to actively corrupt cellular ubiquitin-dependent processes to suppress innate antiviral responses and promote viral replication. DUBs have now been identified in diverse viral lineages, and their characterization is providing valuable insights into virus biology and the role of the ubiquitin system in host antiviral mechanisms. Here, we provide an overview of the structural biology of these fascinating viral enzymes and their role innate immune evasion and viral replication.

Viruses and the Ub System

Viruses have had a significant impact on society throughout history, and it is only since we have started to understand how they establish infection and how they interact with their hosts that we have been able to develop the means to control the diseases they cause. Although viruses depend on the molecular machineries of their host cells for replication, they also express their own specialized replication enzymes to support the production of new virus particles and the spread of infection. Not only do they have to find ways to exploit the cellular machinery they need to establish infection (while often competing with the interests of the cell) but they also have to deal with elaborate antiviral mechanisms that are triggered immediately upon entry of viral material into the cell. Many of these challenges are met by specialized viral enzymes that hijack or manipulate critical cellular systems, and it is therefore not surprising that the study of viruses has repeatedly led to insights into the biology of the cell itself, since viruses have had to "learn" how the cell works in order to survive.

One of the important cellular machineries that is manipulated by viruses is the ubiquitin (Ub) system. Ubiquitination involves the covalent attachment of the C-terminal Gly76 residue of Ub *via* an isopeptide bond to the ε-amino group of a Lys residue or the α-amino group of the N-terminal residue of a protein substrate [1]. Ub is a small, 76-aa protein that is highly conserved, stable, structured, and ubiquitously expressed in virtually all cell types. It adopts a β-grasp fold, consisting of a mixed β-sheet structured around a central α-helix, and harbors a C-terminal diGly motif (Fig. 1A). An exposed hydrophobic patch is centralized around residue Ile44 (frequently referred to as the Ile44 patch) and often facilitates recognition by Ub-binding domains (Fig. 1A) [2,3]. The process of Ub conjugation to substrates is regulated by the E1, E2, and E3 enzymatic cascade leading to (multi)monoubiquitination or formation of polyUb chains upon the modification of a substrate-attached Ub at its Met1, Lys6, Lys11, Lys27, Lys29, Lys33, Lys48, or Lys63 residue [1,4,5]. PolyUb chains can be homogeneous when Ub is attached to the same lysine residue on each Ub in the chain; however, mixed-linkage polyUb chains and

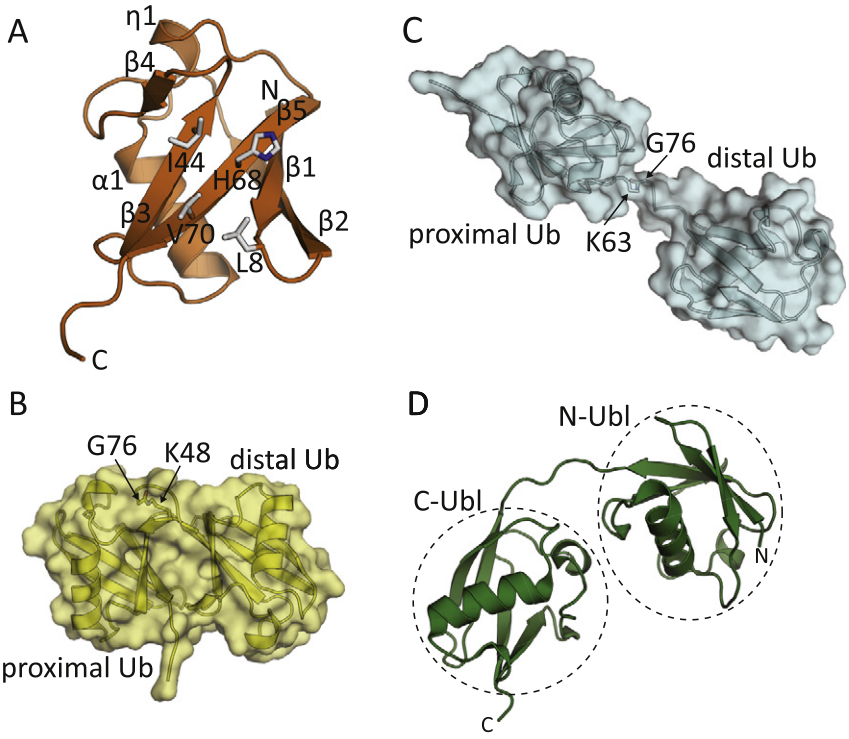

Fig. 1. Structure of Ub and ISG15. (A) Ub (PDB ID: **1UBQ**) is shown in cartoon representation, with the residues forming the Ile44 patch shown as sticks. (B) Crystal structure of the compact, Lys48-linked diUb (PDB ID: **1AAR**) is shown as a cartoon with transparent surface, with the isopeptide bond between Lys48 and Gly76 indicated. (C) Crystal structure of the extended, Lys63-linked diUb (PDB ID: **2JF5**) is shown as a cartoon with transparent surface, with the isopeptide bond between Lys63 and Gly76 indicated. (D) Crystal structure of ISG15 (PDB ID: **1Z2M**) is shown as cartoon, with the N- and C-terminal UBL domains indicated. All structural images were generated using PyMOL [257].

branched Ub chains can also be formed [6]. Classically, Lys48-linked chains adopt compact conformations (Fig. 1B) and play an important role in proteasomal degradation, whereas Lys63-linked chains adopt an extended conformation (Fig. 1C) and have been implicated in positively mediating signal transduction [1]. Both types of ubiquitination are involved in regulating the signaling that directs the antiviral innate immune response [7,8]. Additional Ub-like (UBL) proteins such as SUMO or NEDD8 are structured around a β-grasp fold and possess a C-terminal diGly motif similar to Ub, which allows for covalent conjugation to substrates by their respective E1, E2, and E3 enzymes [9–11]. In contrast, the UBL protein interferon (IFN)-stimulated gene (ISG) 15 (ISG15) is composed of two tandem UBL folds that are connected by a short linker; however, it retains the distinctive diGly motif at its C terminus for attachment to target proteins (Fig. 1D). While ISG15 conjugation has been shown to mediate protection from a number of viruses in mice (reviewed in Refs [12,13]), its role in antiviral immunity remains poorly understood. Interestingly, human ISG15 deficiencies do not appear to alter susceptibility to viral infections [14], and curiously, soluble ISG15 in fact appears to downregulate IFN signaling [15].

The ubiquitination process is highly dynamic and reversible, allowing cells to regulate signal transduction pathways as a response to different stimuli such as virus infections. Deubiquitinating enzymes (DUBs) catalyze the removal of Ub or UBLs from cellular substrates, resulting in either complete deubiquitination or editing/trimming of Ub chains [16]. Around 100 human DUBs can be classified into 5 major families based on their catalytic mechanism and structural features [16,17]. The majority of DUBs are cysteine proteases, which contain an active-site catalytic dyad composed of a Cys nucleophile and a His base arranged in close proximity. The His appears to activate the Cys nucleophile by lowering the pK_a of the side chain and stabilizing the negatively charged thiolate [16]. Often, a third polar residue is present, which likely helps orient the His residue appropriately to facilitate activation of the nucleophile [16]. The Cys protease DUB families include Ub-specific proteases (USPs), ovarian tumor proteases (OTUs), Ub C-terminal hydrolases, and Machado–Joseph disease proteases, whereas the fifth family of DUBs consisting of JAB1/MPN/MOV34 (JAMM) are metalloproteases. More than half of the human DUBs belong to the USP family and generally cleave all Ub linkage types without a clear preference [18]. This is in contrast to the 16

human OTU DUBs that hydrolyze defined subsets of Ub linkage types [19].

Almost all important cellular processes are regulated (in part) by ubiquitination. Whether it is, for example, gene expression, protein trafficking, protein degradation, autophagy, cell cycle progression, programmed cell death, cell survival, or innate immune response, all are regulated by Ub and/or UBLs, either positively or negatively or both. As viruses are extensively using or dealing with some, if not all, of these processes during infection, it is not surprising that several interactions between viruses and the Ub(-like) system in the context of these kinds of cellular processes have been identified. These interactions have been reviewed from several different perspectives by others [20–29]. In particular, however, from all these data, it has become apparent that Ub-mediated regulation of the antiviral innate immune response may be one of the most important targets of viral manipulation.

Antiviral Innate Immune Response and Its Regulation by Ub

The innate immune system of host cells is triggered upon infections with pathogens such as parasites, bacteria, and viruses. In the case of viruses, sensing of viral proteins or specific forms of viral nucleic acid will initiate the activation of the innate immune response leading to expression of antiviral molecules, including IFNs, pro-inflammatory cytokines, and chemokines [30]. Type-I IFNs (IFN-α/β) will induce an antiviral state by upregulating the expression of hundreds of ISGSs in infected and neighboring cells to limit virus replication and spread [31]. Furthermore, the adaptive immune system becomes activated, promoting antigen presentation and developing effective T- and B-cell responses that may ultimately result in clearance of the virus. Excessive activation of the innate immune system can, however, cause chronic inflammation and autoimmune disorders [32], and antiviral signaling pathways are therefore strictly regulated. Key mechanisms that trigger and fine-tune these immune responses in eukaryotes are the post-translational phosphorylation and ubiquitination of cellular immune factors, which can alter their interaction, localization, stability, or activity (Fig. 2) [7,8,33–35].

The first step of the innate immune response is the detection of pathogen-associated molecular patterns by a large repertoire of pattern-recognition receptors (PRRs) present on immune and non-immune cells. On the surface, and in endosomal compartments of immune cells, toll-like receptors (TLRs) play an important role as viral PRRs. Subsequent signaling is directed *via* MyD88, TIR-domain-containing adaptor-inducing IFN-β (TRIF), interleukin-1 receptor-associated kinase 1 (IRAK1) and 4, and receptor-interacting protein 1 (RIP1), ultimately leading to the production of type-I IFNs. Intracytosolic sensors for the detection of viral nucleic acids in virtually all cells are retinoic acid-inducible gene I (RIG-I)-like receptors (RLRs), NOD-like receptors, and viral DNA sensors [cyclic-GMP-AMP (cGAMP) synthase (cGAS) and IFI16 are the key sensors] [36,37]. RIG-I-like receptors include RIG-I and melanoma differentiation factor 5 (MDA5), which bind different forms of viral RNA leading to their activation and oligomerization that will induce the interaction with mitochondrial antiviral signaling protein (MAVS). MAVS recruits signaling molecules such as E3 ligases of the tumor necrosis factor (TNF) receptor-associated factor (TRAF) protein family to activate kinase complexes. TRAF6 will recruit the TAK complex that will phosphorylate the inhibitor of NF-κB kinase γ (IKKγ) [also known as NF-κB essential modulator (NEMO)], which in turn will form a complex with IKKα/β. This complex will initiate the degradation of the NF-κB inhibitor IκBα, which frees NF-κB to promote transcription of pro-inflammatory cytokines. Another protein recruited to MAVS, TRAF3, activates a complex comprising of TRAF family member-associated NF-κB activator (TANK)-binding kinase 1 (TBK1)/IKKε to phosphorylate IFN regulatory factor (IRF) 3 and IRF7. Phosphorylation enables the IRF transcription factors to dimerize and induce the expression of type I IFNs in concert with NF-κB [30,35]. Secreted IFN-α/β will bind to IFN receptors and activate the Janus kinase–signal transducer and activator of transcription pathway, resulting in the transcription of ISGs. ISG-encoded proteins, including ISG15, have antiviral activity by interfering with processes like viral replication or translation [31]. With respect to the detection of DNA viruses, virus-derived cytosolic DNA binds to sensor cGAS, which stimulates the synthesis of cGAMP [38]. cGAMP then activates the stimulator of IFN genes (STING), a membrane-bound protein on the endoplasmic reticulum, which recruits TBK1 and initiates IRF3-mediated transcription of type I IFNs and pro-inflammatory cytokines.

Activation of innate immune signaling is regulated, besides by phosphorylation, through ubiquitination performed by specialized E3 ligases such as the members of the family of TRIM E3 ligases [39]. These and several other E3s conjugate Lys63-linked and Lys48-linked Ub chains to RIG-I, MAVS, TBK1, and STING, as well as MyD88, TIR-domain-containing adaptor-inducing IFN-β (TRIF), interleukin-1 receptor-associated kinase 1 (IRAK1), and receptor-interacting protein 1 (RIP1), while TRAF3 and 6 induce their Lys63-linked auto-ubiquitination, which triggers activation [7,8,35]. IκBα is degraded by the proteasome after Lys48-linked Ub chains are conjugated, which enables downstream signaling [40]. Atypical Ub chains also play a role in the activation of the innate immune response since NEMO is a substrate for conjugation by Lys27, Lys29, and linear polyUb chains, and STING can be modified with Lys11 and

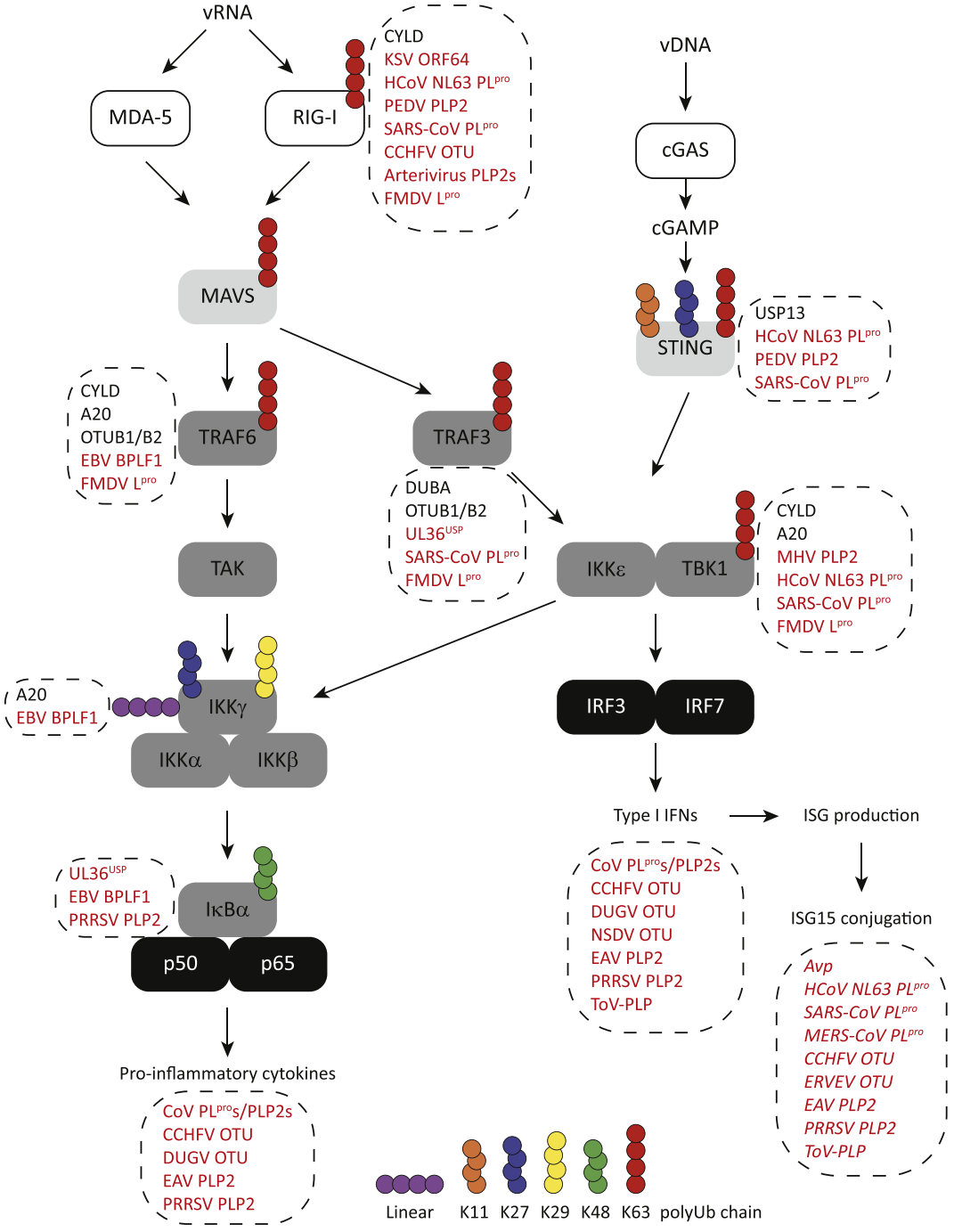

Fig. 2. Illustration of the activation of the innate immune response and its manipulation by human or viral DUBs. White boxes highlight the cytoplasmic receptors RIG-I, MDA5, and cGAS that can sense viral RNA or DNA *via* adaptor proteins MAVS or STING, in light gray, which in turn activate kinase complexes (partly depicted in dark gray). Ultimately, transcription factors IRF3, IRF7, p50, and p65 (black boxes) are activated and translocate to the nuclease to induce the transcription of type I IFNs and pro-inflammatory cytokines. Differently linked polyUb chains involved in the activation of the innate immune response are shown by the different colored polyUb chains. Dashed boxes placed next to innate immune signaling factors contain human or viral DUBs that remove Ub chains from these specific targets. DUBs placed below the type I IFN or NF-κB pathway (inducing the expressing of pro-inflammatory cytokines) interfere with these pathways without knowing their exact substrate(s). Human DUBs are shown in black, vDUBs in red, and vDUBs having deISGylating activity in red italic.

Lys27 polyUb chains [41,42]. Besides conjugated Ub, unanchored Ub chains (Lys63- or Lys48-linked) also seem to play a role in the regulation of innate immune signaling by providing a multimeric scaffold for the activation of RIG-I and MDA-5 complexes [43–45]. In addition, ubiquitination of IRF3 has been observed and implicated in the induction of cellular proapoptotic pathways [46] and in the negative regulation of IFN-β signaling [47].

Negative regulation of the innate immune response is achieved by conjugation of Lys48-linked polyUb to degrade signaling factors and thereby dampen the expression of type I IFNs and pro-inflammatory cytokines. Additionally, actions of E3 ligases that attach different Ub linkage chains can be counteracted by several specific cellular DUBs [7,48]. CYLD (USP) is able to cleave linear and Lys63-linked Ub chains, and it deubiquitinates RIG-I, TRAFs, and TBK1 [49]. OTUB2 (an OTU domain containing DUB) removes Lys63-linked Ub chains from TRAF3 and TRAF6, as does OTUB1; however, *in vitro*, this latter enzyme preferentially cleaves Lys48-linked Ub chains [19]. Interference with the Lys63-linked auto-ubiquitination of TRAF3 is performed by DUBA (OTUD5), which interacts with TRAF3 [50]. A20 is a complex regulator since it contains an OTU domain at its N terminus that cleaves Lys63-linked polyUb chains and a C-terminal E3 ligase domain for conjugating Lys48-linked Ub [51,52]. Deubiquitination of TRAF6 and NEMO by A20 leads to suppression of NF-κB activation. A20 also disrupts the activation of TBK1 complexes containing TRAF3; however, the interference mechanism is unknown [53]. Additionally, A20 can also bind to specific E2 enzymes and induce their degradation as a mechanism to prevent ubiquitination of other proteins [54]. Several more DUBs that play a role in the regulation of the immune response have been identified such as OTU DUBs Cezanne, OTULIN, and UPS DUBs USP3, 13, and 21 [7,55–58]. Mutations in genes encoding DUBs involved in negative regulation of innate immune signaling, like CYLD and A20, can lead to the development of diseases including cancer and autoimmune and inflammatory disorders, highlighting the importance of DUB-controlled immune signaling [59,60].

Virus-Encoded DUBs

Constant interactions between hosts and pathogens shape both the cellular antiviral system (in order to efficiently eliminate invading pathogens) and the pathogens (that will evolve and adapt to facilitate efficient replication of their genomes) [61]. Particularly viruses with an RNA genome have a high mutation frequency, which is triggered by the lack of proofreading activity in the viral RNA polymerases that drive their replication [62]. As a result, virus populations are genetically diverse, enabling them to rapidly adapt to changing circumstances. This also enables viruses to acquire diverse genes from various sources or evolve viral enzymes to expand their activities [63]. Mechanisms to avoid or delay the activation of the innate immune system are exploited by viruses to manipulate the host cell environment [64,65]. Modifying Ub signaling to evade the activation of the innate immune response is used by both DNA and RNA viruses, and methods include, for example, blocking activity or hijacking host E3 ligases or DUBs [66]. Another elaborate viral approach is the expression of virus-encoded E3 ligases or DUBs that can suppress the innate immune response but also potentially affect many other Ub-dependent signaling pathways in the host [66–68]. In this review, we focus on virus-encoded DUBs (listed in Table 1) that have been identified in DNA viruses (adeno- and herpesviruses) and RNA viruses (corona-, arteri-, nairo-, picorna-, and tymoviruses), with an emphasis on the structural biology of these viral DUBs (vDUBs) and their (potential) innate immune suppressive mechanisms.

Adenoviridae

Adenoviruses (AdVs) are non-enveloped, double-stranded DNA viruses, with their genomes encapsulated in an icosahedral protein shell. Infection by human AdV generally causes mild respiratory disease, although life-threatening disease can occur in immunocompromised individuals. The ability of AdV infection to efficiently stimulate cellular and humoral immune responses, coupled with the relative ease of genetic manipulation and large genome size, has led to their intensive investigation as gene delivery vectors [69].

Following virus entry and the onset of genome replication, AdVs rely on the expression of late genes that are primarily responsible for the production of structural proteins involved in virion assembly [70]. Following assembly, capsid proteins are proteolytically processed, yielding infectious viral particles, a feat accomplished through the activity of the AdV cysteine protease Avp [71]. Initial efforts characterizing Avp determined consensus sequences of (M,L,I)XGX↓G and (M,L,I)XGG↓X [72], and further studies identified two viral co-factors that are required for recombinant Avp activity *in vitro*: AdV DNA and an 11-aa peptide derived from the C terminus of the Avp substrate precursor protein pVI (pVIc) [73].

During viral infection, antigen presentation *via* cellular major histocompatibility complex class I is reliant on the degradation of viral peptides *via* the Ub-proteasome system, and a number of viruses have been found to interfere with this process. Upon observing a reduction in Ub-conjugated proteins in AdV-infected cells, Balakirev and coworkers hypothesized that Ad may employ a vDUB to interfere with cellular Ub-dependent processes [74]. Using reversible Ub-based probes, Avp was identified as an AdV

Table 1. Viral DUBs and their characterized structures and substrates

Virus family/genus	Virus	DUB domain	Location	*In vitro* DUB activity	Cellular targets	PDB ID
Adenoviridae	AdV	Avp	L3 gene product p23	Lys48 polyUb, ISG15 [74]	Histone H2A [74]	1AVP, 1NLN, 4EKF, 4PID, 4PIE, 4PIQ, 4PIS, 5FGY, 4WX4, 4WX6, 4WX7
Herpesviridae/ alphaherpesviruses	Human HSV-1	UL36^{USP}	N terminus of viral tegument protein	Lys48 polyUb [85,86], Lys63 polyUb [86]	TRAF3 [88], IκBα [89]	
	MDV	MDV^{USP}		N/A	Unknown	
	PrV	pUL36		N/A	Unknown	
Herpesviridae/ betaherpesviruses	MCMV	M48^{USP}	N terminus of viral tegument protein	Lys48/63 diUb [91]	Unknown	2J7Q
	HCMV	UL48^{USP}		Lys48/63 polyUb [86]	Unknown	
Herpesviridae/ gammaherpesviruses	EBV	BPLF1	N terminus of viral tegument protein	Lys48/63 polyUb [94], NEDD8 [95]	EBV RR [94], proliferating cell nuclear antigen [98], Cullin [95], TRAF6 [99,100], NEMO, IκBα [100]	
	KSV	KSV Orf64		Lys48/63 polyUb [103]	RIG-I [105]	
	MHV-68	ORF64^{USP}		N/A	Unknown	
Coronaviridae/ alphacoronaviruses	HCoV-NL63	HCoV-NL63 PLP2	Membrane- associated nsp3 that is part of the replication–transcription complex	Lys48/63 polyUb [138,172], ISG15 [173]	RIG-I, TBK1, IRF3, STING [174]	
	PEDV	PEDV PLP2		N/A	RIG-I, STING [183]	
	TGEV	TGEV PL1^{pro}		Lys48/63 polyUb [182]	Unknown	3MP2
Coronaviridae/ betacoronaviruses	SARS-CoV	SARS-CoV PL^{pro}	Membrane-associated nsp3 that is part of the replication–transcription complex	Lys48 polyUb [130,139,158], Lys63 polyUb [158], ISG15 [130,158], Lys6/11/27/29/33/48/63 diUb [139]	RIG-I, TRAF3, STING, TBK1, IRF3 [256]	4M0W, 5E6J, 3E9S, 3MJ5, 4MM3, 4OVZ, 4OW0, 2FE8, 5TL6, 5TL7
	MERS-CoV	MERS-CoV PL^{pro}		Lys6/11/29/33/48/63 diUb [139], Lys48 polyUb [139,158,162], Lys63 polyUb [158,162], ISG15 [158]	Unknown	4P16, 4PT5, 4R3D, 4REZ, 4RF0, 4RF1, 4RNA, 4WUR
	MHV	MHV PLP2		Lys11/48/63 diUb [177]	IRF3 [179], TBK1 [178]	4YPT
Coronaviridae/ gammacoronaviruses	IBV	IBV PL^{pro}	Membrane- associated nsp3 that is part of the replication–transcription complex	Lys48/63 polyUb [188,189]	Unknown	4X2Z 5BZ0
Arteriviridae	EAV	EAV PLP2	N-terminal region of membrane-associated nsp2 that is part of the replication–transcription complex	Lys48/63 polyUb [196]	RIG-I [196]	4IUM
	PRRSV	PRRSV PLP2		Lys6/11/27/29/33/48/63 diUb, Lys48/63 polyUb [209]	IκBα [208], RIG-I [196]	
	LDV	LDV PLP2		N/A	RIG-I [196]	
	SHFV	SHFV PLP2		N/A	RIG-I [196]	
Bunyaviridae/ nairoviruses	CCHFV	CCHFV OTU	N-terminal region of RNA-dependent RNA polymerase-containing L-segment	Lys48/63 polyUb [198,219,221], ISG15 [198,217–219,221], Lys6/11 diUb [221], Lys63 diUb [218,219,221],	RIG-I [196]	3PHU, 3PHW, 3PHX, 3PT2, 3PSE, 3PRM, 3PRP

Table 1 (*continued*)

Virus family/genus	Virus	DUB domain	Location	*In vitro* DUB activity	Cellular targets	PDB ID
				Lys48 diUb [219,221]		
	DUGV	DUGV OTU		Lys48/63 polyUb [198,219,221], ISG15 [198,217–219,221], Lys6/11 diUb [221], Lys63 diUb [218,219,221], Lys48 diUb [219,221]	Unknown	4HXD, 3ZNH
	ERVV	ERVEV OTU		ISG15 [221]	Unknown	5JZE
	NSDV	NSDV OTU		N/A	Unknown	
Picornaviridae	FMDV	FMDV L^{pro}	N terminus of polyprotein	Lys48/63 polyUb [240]	RIG-I, TBK1, TRAF3, TRAF6 [240]	1QOL, 4QBB, 1QMY
	G	ToV-PLP	2C/3A junction of the *Enterovirus* G polyprotein	Met1/Lys48/63 polyUb, ISG15 [226]	Unknown	
Tymoviridae	TYMV	TYMV PRO	Non-structural protein p206	Lys48/63 polyUb [221,250]	TYMV p66 [250]	4A5U

DUB capable of cleaving Lys48-linked tetra Ub chains and ISG15, thus providing the first example of a viral protease with deubiquitinating activity [74]. Indeed, the demonstration of Avp DUB activity would be supported by the compatibility of the previously elucidated Avp consensus sequences with the C-terminal LRGG motif of Ub [72]. The study also demonstrated a significant reduction in the cellular levels of ubiquitinated histone H2A in AdV-infected HeLa cells, suggesting a potential ubiquitinated cellular target for Avp.

Ding and coworkers provided the first structural insights into Avp, crystallized in the presence of pIVc (Fig. 3A) [75]. The structural complex revealed similarities with the archetypal cysteine protease papain, which contains a β-sheet "right" (R) and α-helical "left" (L) subdomain that pack together to form a cleft that leads toward the active site (Fig. 3B and C) [76]. The Avp active site is composed of residues His54, Glu71, and Cys122, which superpose closely with the catalytic triad of papain (Fig. 3D). A fourth residue, Gln115, is also present and proposed to participate in the formation of the oxyanion hole, which stabilizes the negatively charged tetrahedral intermediates that form during peptide bond hydrolysis. Later studies describing the structure of Avp in the absence of pVIc concluded that pVIc repositions a loop carrying active-site residue His54 to orient the residue toward an optimal geometry for catalysis (Fig. 3A) [77]. The activating peptide pIVc binds Avp by forming a disulfide bridge with the β-sheet lobe of Avp and forming the sixth strand of the core β-sheet structure (Fig. 3A).

Despite the similarities between Avp and papain, their primary structures differ significantly, with the catalytic triad residues appearing in the order His-Glu-Cys in the case of Avp, compared to Cys-His-Asn in the case of papain. This prompted the establishment of a novel cysteine protease group (currently categorized as a clan CE protease within the MEROPS database) with Avp proposed as an exemplary case of convergent evolution [75]. It has been noted, however, that proteins with rearranged amino acid sequences, yet similar three-dimensional structure, may be related by circular permutation, which would suggest a common origin [78].

Currently, there is no direct structural evidence for the activation of Avp by DNA, although attempts at modeling these interactions have been made [79]. Further structural work may be able to shed light on these questions. The implications of pVIc binding and Avp activation, however, are clearer, and it has been suggested that rational, structure-based efforts could guide the development of novel peptide-based inhibitors of Avp as a treatment for AdV infection [75].

Herpesviridae

Herpesviruses are large DNA viruses, with double-stranded DNA genomes ranging from 124 to 295 kb [259]. The *herpesviridae* family consists of a subset of viruses within the order *Herpesvirales* that infect mammals, birds, and reptiles [259]. The *herpesviridae* family is further divided into subfamilies, namely the *alpha*-, *beta*-, and *gammaherpesvirinae*, on the basis of shared biological characteristics. The herpesvirus virion structure is composed of an icosahedral

nucleocapsid hosting the viral genome, which is surrounded by the viral matrix, or tegument, and contained within the viral envelope. All herpesviruses can establish lifelong infections in their respective hosts, remaining latent until periods of reactivation.

A number of herpesviruses are important human pathogens. Primary infection by herpes simplex virus 1 (HSV-1) causes cold sores, which is followed by a period of latency where the virus remains dormant within sensory neurons awaiting reactivation. Reactivation can be provoked *via* a number of external stimuli, allowing for viral replication and transmission to resume [80]. Epstein–Barr virus (EBV) was the first recognized tumor-causing virus to infect humans and has been associated with a number of diseases affecting B-cells, including Burkitt's Lymphoma, as well as Hodgkins and non-Hodgkins lymphomas [81].

Several examples of herpesviral DUBs are described below, which are all homologs of each other. Herpesviruses have large genomes, and some may code for up to three different DUBs [82], which emphasize the apparent importance of DUB activity to these viruses [20].

HSV-1 UL36^{USP}

Seminal work by Borodovsky and coworkers provided a means to rapidly identify DUBs from cellular extracts [83]. Using intein-mediated chemical ligation, Ub derivative substrates were fashioned to contain a thiol-reactive group in place of the C-terminal Gly76 residue, which, when exposed to a catalytically competent DUB, formed a covalent linkage between the Ub-based probe and the active-site thiol of the target enzyme [83]. The resulting adducts could then be immunoprecipitated and identified by mass spectrometry [83,84]. Using their probes, an Ub-reactive ~47-kDa product was identified in lysates of cells infected with HSV-1 [85]. The product was mapped to the N terminus of the HSV-1 gene product expressed from the UL36 open reading frame (ORF) and was subsequently termed UL36^{USP} on the basis of its reactivity with Ub [85]. Interestingly, the UL36 ORF encodes for a 3164-aa tegument protein, and the identification of a 47-kDa HSV-1 gene product clearly indicated the occurrence of a post-translation cleavage event, although the enzyme responsible for this cleavage remains unknown. UL36^{USP} was found to be

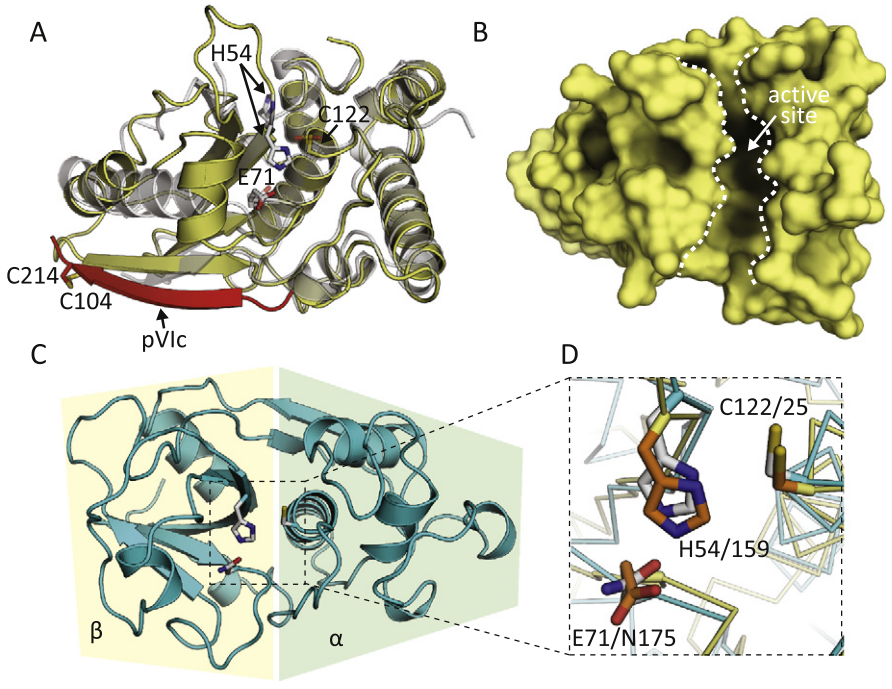

Fig. 3. Crystal structure of adenovirus Avp. (A) Superposition of Avp bound to activating peptide pVIc (PDB ID: **1AVP**; yellow and red, respectively) and Avp in the absence of pVIc (PDB ID: **4EKF**; transparent gray). Active site residues are shown as sticks in both structures, and the disulfide bridge between Avp and pVIc is indicated. (B) Surface representation of Avp (PDB ID: **1AVP**). Dashed white lines highlight the active-site cleft. (C) Crystal structure of papain (PDB ID: **1PPN**). The left (L) α-helical domain and right (R) β-sheet domain are indicated by green and yellow boxes, respectively. (D) Superposition of the active-site residues of Avp (yellow) and papain (cyan). Active site residues of papain are shown as gray sticks, and those of Avp are shown as orange sticks. Avp residues are indicated, followed by the equivalent residues of papain. Papain and Avp structures were aligned using the SPalign-NS server [258].

active toward both Lys48- and Lys63-linked polyUb chains, with a preference for Lys63 linkages [85,86].

Infection by herpesviruses is detected by different PRRs; however, herpesviruses are able to evade detection by the innate immune system to establish persistent infections [87]. Wang *et al*. demonstrated that the ectopic expression of UL36^{USP} decreased Sendai virus-mediated production of IFN-β, indicating that UL36^{USP} is involved in the modulation of cellular innate immune signaling pathways [88]. To probe the role of UL36^{USP} during an infection, the authors used an HSV-1 bacterial artificial chromosome system to generate recombinant HSV-1 with a catalytically inactive UL36^{USP} (Cys40Ala). Infections with the UL36^{USP} knockout virus resulted in increased production of IFN-β, while virus containing wild-type UL36^{USP} impaired cellular IFN-β production, demonstrating that UL36^{USP} is an IFN antagonist [88]. To further elucidate the role of UL36^{USP}, reporter assays confirmed that UL36^{USP} interfered with IFN-β promoter activation at a level between MAVS and TBK1, possibly *via* deubiquitination of TRAF3, and inhibited the activity of both IRF- and NF-κB-responsive promoters [88]. Later work demonstrated that UL36^{USP} also inhibits NF-κB signaling at a level between IKK and p65 [89]. Consistent with this observation, expression of UL36^{USP} resulted in a reduction in the levels of Ub-conjugated IκBα [89].

UL36^{USP} also demonstrated a role in interfering with the STING pathway involved in detection of cytoplasmic viral DNA. UL36^{USP} inhibited cGAS/STING mediated activation of IFN-β and NF-κB-responsive promoters, and reduced production of IFN-β and IL-6 mRNA transcripts [89], presumably through deubiquitination of IκBα.

MCMV M48^{USP}

Homologs of UL36^{USP} are predicted to exist among all members of the herpesviridae family on the basis of sequence similarity and the absolute conservation of putative catalytic Cys and His residues [90]. Indeed, Schlieker *et al*. confirmed the DUB activity of the homologs murine cytomegalovirus (MCMV) M48^{USP} domain using a fluorogenic Ub substrate [90] and later Lys48- and Lys63-linked diUb and cellular Ub conjugates [91]. Subsequent determination of the crystal structure of the enzyme bound to Ub vinylmethylester offered the first insights into the structure of a herpesvirus DUB (Fig. 4) [91]. M48^{USP} shares little overall structural similarity to other cysteine proteases of known structure. It consists of a central β-sheet sandwiched between two α-helical domains, and the authors proposed M48^{USP} to be a member of a novel class of DUBs, termed herpesvirus tegument USPs. Importantly, the M48^{USP}–Ub structure revealed how the vDUB recognizes Ub. The C-terminal extension of Ub binds into a cleft formed between the β-sheet and an α-helical subdomain of M48^{USP}, and recognition of the hydrophobic Ile44 patch of Ub is facilitated by a unique β-hairpin extending from an eight-stranded β-sheet of the M48^{USP} core (Fig. 4).

Perhaps the most striking feature of M48^{USP} is the organization of its catalytic triad. While residue His141, the predicted general base, is spatially conserved with respect to the active site of most papain-like proteases (PLPs), mutational analysis suggested that His158, also positioned near the Cys nucleophile, could act as a catalytic base, although the authors cautioned that both His residues might participate in catalysis (Fig. 4) [91]. In addition, a glutamine (Gln10) residue near the active site was suggested to contribute to the formation of the oxyanion hole, due to its position and strict conservation throughout homologous herpesvirus proteases.

Investigations into the role of M48^{USP} *in vivo* have shown that abrogating the catalytic activity of the vDUB results in significantly attenuated MCMV replication in mice [92]. This replication deficiency *in vivo* was attributed in part to increased levels of MCK2, an MCMV-encoded pro-inflammatory chemokine [92]. M48^{USP} was postulated to be responsible for the careful regulation of MCK2 production and secretion in a mechanism at least partially dependent on proteolytic activity, as evidenced by the accumulation of unglycosylated MCK2 in infected cells but not with M48^{USP} mutant virus, further emphasizing the critical role of vDUBs in regulating inflammatory processes, and by the requirement that these processes be carefully controlled to facilitate productive infection [92]. While these efforts have provided valuable insight toward the role of M48^{USP} during infection, the specific targets of the vDUB remain to be determined.

EBV BPLF1

Concomitant with the discovery of MCMV and HSV-1 DUBs, a bona fide deubiquitinase was identified in EBV, a representative of the gammaherpesvirus subfamily [90]. Earlier studies using yeast two-hybrid screens identified the interaction of BPLF1, a UL36^{USP} homolog, with the EBV ribonucleotide reductase (RR) [93]. EBV RR is composed of a large (RR1) and small (RR2) subunit, and BPLF1 was shown to reduce cellular levels of ubiquitinated RR1 and thereby inhibit EBV RR activity in a protease-dependent manner. The activity of BPLF1 toward Lys63- and Lys48-linked polyUb partially explained the ability of BPLF1 to inhibit host enzymatic activity *via* Lys63-linked Ub deconjugation [94].

Interestingly, using GFP-based fluorescence cell culture assays, Gastaldello *et al*. identified BPLF1 as a potent deneddylase that could efficiently remove the UBL protein NEDD8 from Cullin, a scaffold protein involved in the formation of Cullin-RING Ub ligases (CRLs) [95]. Cullins are well-characterized NEDD8 substrates, and CRL activity can be dependent on

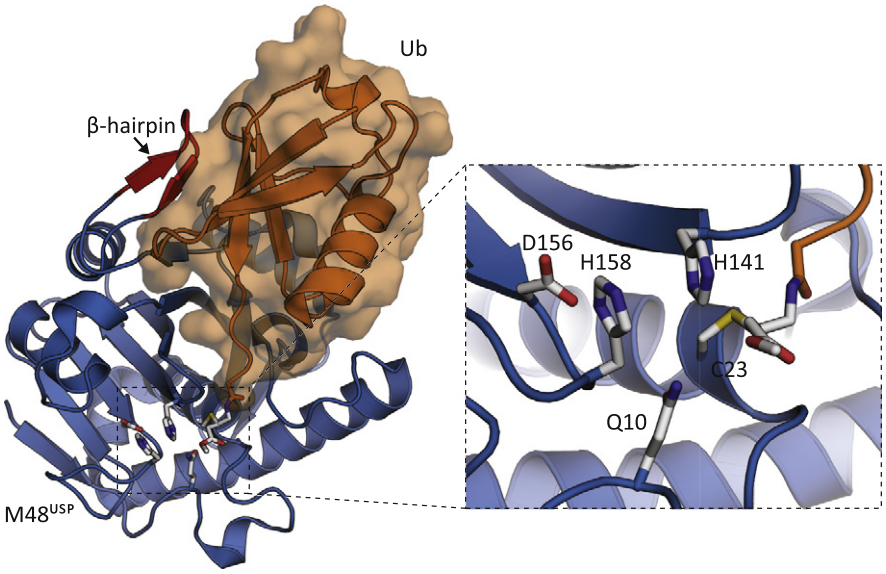

Fig. 4. Crystal structure of MCMV M48^{USP} in complex with Ub. MCMV M48^{USP} (PDB ID: **2J7Q**; blue cartoon) shown in covalent complex with Ub (orange cartoon with transparent surface representation). The unique β-hairpin of M48^{USP} interacting with the Ile44 patch of Ub is colored in red. Dashed box contains a close-up of the M48^{USP} active site, with catalytic residues shown as sticks, including the two catalytic bases His158 and His141. Also shown is Gln10 suggested to take part in the formation of the oxyanion hole.

neddylation [96]. BPLF1-mediated deneddylation stabilized CRL substrates, likely *via* inhibition of CRL-mediated ubiquitination. Of these stabilized substrates, CDT1, a cellular licencing factor required for DNA replication and entrance into S-phase, was found to be required for EBV replication [95]. EBV BPLF1 was thus found to stabilize host factors critical for the establishment of a cellular environment permissive to EBV replication. Subsequent characterization of an EBV ΔBPLF1 virus revealed it to have severely reduced infectivity and delayed transformation of B-cells [97].

In addition to a role in cell cycle regulation, expression of BPLF1 has been shown to reduce the monoubiquitination of proliferating cell nuclear antigen (PCNA) and prevent polymerase recruitment during DNA damage repair [98]. Furthermore, BPLF1 has been implicated in the inhibition of the host innate immune response to viral infection. Saito and co-workers demonstrated that overexpression of BPLF1 reduced the cellular levels of ubiquitinated TRAF6, inhibiting NF-κB activation and promoting viral replication [99], while others have shown BPLF1 to inhibit TLR signaling likely *via* deubiquitination of downstream signaling components [100]. Besides BPLF1, EBV may express two other proteins with DUB activity, BSLF1 and BXLF1, but further investigation into their relevance is necessary [82].

Additional DUBs in the Herpesviridae family

Homologs of UL36^{USP} with confirmed deubiquitinating activity have been identified in human cytomegalovirus (HCMV), murine gammaherpes virus 68 (MHV-68), Marek's disease virus (MDV), and Kaposi's sarcoma virus (KSV) [101–104]. UL48^{USP} and ORF64^{USP} from HCMV and KSV, respectively, were both found to process Lys48- and Lys63-linked polyUb chains *in vitro* [86,103], and KSV ORF64^{USP} was found to target RIG-I, thereby inhibiting IFN-β and NF-κB promoter activity [105]. Recombinant viruses harboring active-site mutations within their respective DUB domains have shed light on the role of herpesvirus DUBs *in vivo*. KSV virus with an active-site mutation in ORF64^{USP} implicated its DUB activity in the lytic replication cycle [103], while recombinant MDV with a catalytically inactive MDV-^{USP} implicated DUB activity in the maintenance of cellular transformation *in vivo* [104]. Furthermore, an HCMV UL48^{USP} active-site mutant decreased the production of infectious viral progeny during infection [101]. Finally, while the DUB activity of the pseudorabies virus (PrV) pUL36 domain has yet to be confirmed *in vitro*, infection with a recombinant virus containing a Cys-Ser mutation at the catalytic nucleophile of pUL36 demonstrated delayed neuroinvasion in mice [106]. Further investigation into the role of pUL36 *in vivo* using quantitative mass spectrometry identified Lys442 as a conserved and critical ubiquitination site on pUL36, with increased modification observed during infection with the catalytically inactive mutant virus [107]. pUL36 was proposed to act as a Ub switch, with ubiquitination/deubiquitination at Lys442 controlling invasive states of PrV, and with pUL36 DUB activity and Lys442 ubiquitination acting as critical factors for neuroinvasion and retrograde axonal transport, respectively [107].

Coronaviridae

Coronaviruses (CoVs) are enveloped viruses within the order Nidovirales with the largest known positive-sense single-stranded RNA (ssRNA) genomes (26–34 kb). They are grouped further into *alpha*-, *beta*-, and *gammacoronavirus* lineages based on sequence similarity [260]. A number of CoVs cause respiratory disease in humans. Notably, in November 2002, a case of atypical pneumonia in Guangdong, China [108] led to the identification of the severe acute respiratory syndrome (SARS) CoV (SARS-CoV) [109–111], which rapidly caused a global pandemic. Ultimately, successful infection control measures brought the SARS-CoV pandemic to an end in July 2003. More recently, in June 2012, a novel CoV was isolated from a 60-year-old male from Saudi Arabia following a fatal case of severe pneumonia and renal failure [112]. This virus, now referred to as Middle East respiratory syndrome (MERS) CoV (MERS-CoV) has since led to 1917 confirmed cases and 684 deaths as of March 2017 [113]. Currently, no MERS- or SARS-CoV-specific therapies exist. Both MERS- and SARS-CoV are expected to have emerged into human populations through animal vectors, with camels and palm civets expected as the primary zoonotic sources, respectively [114,115].

The SARS-CoV outbreak prompted deeper investigation into CoVs as respiratory pathogens, and post-SARS, the human CoV NL63 (HCoV-NL63) was identified, with retrospective analysis suggesting that the virus had been circulating in human populations for some time prior to its discovery [116]. HCoV-NL63 is most closely related to HCoV-229E, which is one of two CoVs identified pre-SARS in the 1960s and recognized as a causative agent of the common cold [117]. HCoV-NL63 has also been associated with croup in young children [118].

CoVs also cause disease in several animals. The neurotropic mouse hepatitis virus (MHV) strains JHM and A59, which group along with SARS-CoV in the *betacoronavirus* genus, cause demyelinating encephalomyelitis in mice and have served as disease models for multiple sclerosis [119]. The porcine transmissible gastroenteritis (TGEV) and porcine epidemic diarrhea virus (PEDV) are *alphacoronaviruses* that cause significant financial burdens in the pork industry [120].

The non-structural proteins (nsps) of CoVs are encoded within two ORFs, ORF1a and ORF1b, with translation yielding polyprotein 1a or 1ab, the latter arising from a −1 ribosomal frameshift that provides access to ORF1b [121]. The CoV polyproteins are post-translationally processed into functional nsps by protease domains encoded within, including a 3C-like cysteine protease ($3CL^{pro}$), which functions as the main protease, and either one or two additional PLPs, which are numbered sequentially according to their position within the polyprotein. In cases where only a single PLP is present, it is referred to simply as PL^{pro}.

SARS-CoV PL^{pro}

Full-length genomic sequences from a number of clinical isolates of SARS-CoV became available shortly after the pandemic [122–124], and their analysis predicted the presence of a single PLP (PL^{pro}) encoded within nsp3 [125]. The absence of a second paralogous PLP domain, combined with an analysis of putative cleavage sites, suggested that PL^{pro} was responsible for cleaving three sites within the SARS-CoV polyprotein and releasing nsp1, nsp2, and nsp3 from the viral polyprotein [125]. This activity was soon confirmed experimentally, with PL^{pro} recognizing the consensus site LXGG [126,127]. Structural modeling of SARS-CoV PL^{pro} based on the crystal structure of the cellular DUB herpesvirus-associated USP (HAUSP) suggested that the viral enzyme adopts a papain-like fold with a circularly permutated C4 zinc finger domain [128]. The structural similarity between PL^{pro} and a cellular DUB, along with the compatibility of the PL^{pro} consensus cleavage sequence with the C-terminal RLRGG motif of Ub, led to the hypothesis that PL^{pro} may possess DUB and possibly ISG15-deconjugating (deISGylating) activity [128].

The *in vitro* DUB [129,130] and deISGylating [130] activities of PL^{pro} were confirmed in parallel by independent groups, demonstrating activity toward Lys48-linked Ub chains. This DUB activity has been implicated in the downregulation of cellular innate immune responses [131], consistent with the observation that SARS-CoV infection prevents IFN-β induction in infected cells [132]. Devaraj and co-workers demonstrated that PL^{pro} inhibited RIG-I-, MDA5-, and TLR3-mediated IFN-β promoter activity and interfered with signaling components specific to IRF3 activation [131]. Interestingly, while their studies showed no effect on NF-κB-dependent transcripts, others found marked reduction in the activity of an NF-κB-responsive promoter in the presence of PL^{pro} [133]. The role of PL^{pro} in the inhibition of IRF3 activation has been further investigated, and it has been suggested to deubiquitinate and inhibit the ability of constitutively active IRF3 to induce IFN-β promoter activity [134].

A crystal structure of SARS CoV PL^{pro} confirmed it to have a domain organization similar to HAUSP, which consists of “thumb”, “palm”, and “fingers” subdomains that organize together to resemble an extended right hand (Fig. 5A) [135,136]. The α-helical thumb and β-sheet palm domains pack together and host a Cys-His-Asp catalytic triad at their interface, with residues adopting a similar geometry to that found in papain, while the fingers domain harbors a circularly permutated C4 zinc finger as had been predicted (Fig. 5A) [128]. Additionally, a tryptophan residue (Trp107) near the active site was found to be oriented such that the indole ring hydrogen was believed to form part of the oxyanion hole (Fig. 5A). Also situated near the active site was a 6-aa loop

flanked by glycine residues. This loop is also present in the cellular HAUSP and USP14, where it is termed blocking-loop 2 (BL2; Fig. 5A), as it occludes the active site of USP14 in the absence of Ub and is thus proposed to serve a regulatory function. In PL^{pro}, this loop is found to be in an "open" state, although molecular dynamics simulations predict that the loop samples both "open" and "closed" conformations [137]. Intriguingly, the N-terminal domain of PL^{pro} adopts a UBL β-grasp fold, which packs against the thumb domain (Fig. 5A). While little is known regarding the function of this domain, conflicting data have been reported showing that this domain is either required [133] or dispensable [138] for the immunomodulatory activity of PL^{pro}, although the UBL domain does not appear to be necessary with respect to DUB activity [133,139].

A crystal structure of a non-covalent SARS-CoV PL^{pro}–Ub complex showed that the C-terminal linear RLRGG peptide extending from the Ub substrate was bound at the interface between the α and β domains in cleft leading toward the active site [140], as previous modeling had predicted [135], with the BL2 loop undergoing significant conformational changes toward the C terminus of Ub [140]. Crystal structures of PL^{pro} bound to the C-terminal domain of human and mouse ISG15 (mISG15) have also now been reported, demonstrating that species-specific recognition of ISG15 molecules is mediated by unique interactions between PL^{pro} and the respective ISG15s [141]. Whether or not PL^{pro} also recognizes the N-terminal domain of ISG15(s) remains to be investigated.

Recently, the structural basis for Lys48-linked polyUb binding of SARS-CoV PL^{pro} was elucidated by the determination of the crystal structure of PL^{pro} in covalent complex with Lys48 diUb [142]. The Lys48 diUb probe was fashioned with a cysteine-reactive alkyne at the C terminus of the proximal Ub moiety, enabling covalent binding of the molecule to PL^{pro} and interaction of its individual Ub domains associated with S1 and S2 binding sites on the vDUB domain (Fig. 5B) (see Ref. [143] for nomenclature). Consistent with earlier predictions [144], the Lys48 diUb probe bound PL^{pro} in an extended conformation, as opposed to the canonical compact conformation observed with most Lys48-linked Ub chains. Binding of the distal Ub moiety at the S2 site was governed by a number of solvent-exposed hydrophobic residues at the surface of an α-helix within the thumb domain, which associated with the Ile44 patch of Ub (Fig. 5B) [142,144]. These studies supported earlier observations that Lys48-linked polyUb chains were processed into diUb moieties, and PL^{pro} may recognize Lys48 diUb preferentially [139].

The involvement of PL^{pro} in the maturation of the viral polyprotein and its role in counteracting cellular antiviral signaling pathways have contributed to its recognition as a promising target for therapeutic intervention, and the availability of X-ray crystallographic data [135,140], along with work describing the substrate specificity of PL^{pro} at its cognate subsites [145,146], has contributed to such efforts. High-throughput screening of small-molecule libraries and rational structure-guided design have led to the identification and development of several lead compounds capable of inhibiting the proteolytic activities of SARS-CoV PL^{pro} [147–154].

MERS-CoV PL^{pro}

Sequencing of the MERS-CoV genome and phylogenetic analysis indicated that the virus shares most recent common ancestry with bat CoVs HKU4 and HKU5 and led to the identification of a single PL^{pro} domain encoded within nsp3 [155]. The polyprotein cleavage sites were initially predicted based on sequence alignment with other CoV polyproteins [155], and PL^{pro} was later confirmed to process sites at the nsp1–2, nsp2–3, and nsp3–4 junctions [156–158]. The *in vitro* DUB activity of PL^{pro} was subsequently confirmed, displaying activity toward mono Ub [139,159–161], Lys48- and Lys63-linked polyUb [139,158,162], Lys6-, Lys11-, Lys29-, Lys33-linked diUb [139], and ISG15 [158]. PL^{pro} was also found to globally deconjugate Ub and ISG15 from cellular targets in cell culture [157,158,162,163].

A crystal structure of the MERS-CoV PL^{pro} domain revealed that the protease adopted a similar fold to SARS-CoV PL^{pro}, with thumb, palm, and fingers subdomains, including the presence of a circularly permutated 4C zinc finger and an N-terminal UBL domain [159,162]. As expected, the active site is composed of a Cys-His-Asp catalytic triad, although interestingly, the oxyanion hole of MERS-CoV PL^{pro} appears deficient. The tryptophan residue proposed to form part of the oxyanion hole in SARS-CoV PL^{pro} is replaced with a leucine, which is unable to participate in stabilizing the oxyanion since its side chain is entirely non-polar. Consistent with this observation, a tryptophan substitution aimed at restoring the MERS-CoV oxyanion hole increased the catalytic activity of PL^{pro} [159,160]. Differences have also been noted in the BL2 loop, which, in the case of SARS-CoV PL^{pro}, was found to interact with small-molecule inhibitors of the enzyme [148,153]. These SARS-CoV-specific compounds are ineffective toward MERS-CoV PL^{pro}, likely due to structural differences in the BL2 loop and the inability of MERS-CoV PL^{pro} BL2 residues to complete analogous hydrogen-bonding and hydrophobic interactions with these compounds [164].

The fact that CoV PL^{pro} domains possess two distinct functions, which comprise both DUB and polyprotein cleavage activities, complicates the ability to study these respective functions exclusively, as both activities depend on the same active site. Studying the role of PL^{pro} DUB activity independent of viral polyprotein processing thus necessitates its

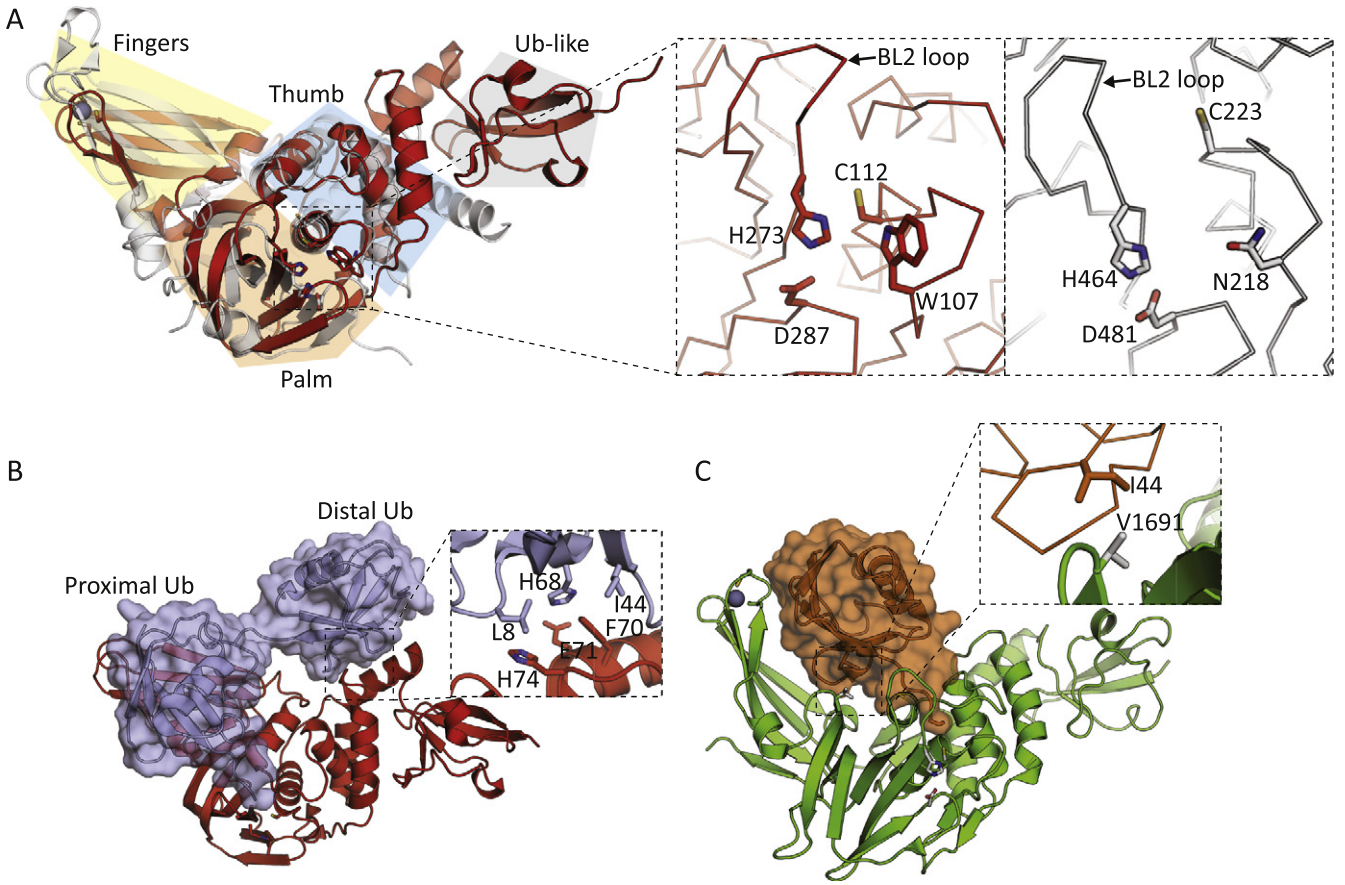

Fig. 5. Crystal structures of zoonotic SARS- and MERS-CoV PL^{pro} domains. (A) Superposition of SARS-CoV PL^{pro} (PDB ID: **2FE8**; red) with HAUSP (PDB ID: **1NB8**; transparent gray). Thumb, fingers, palm, and UBL domains are indicated with blue, yellow, orange, and gray shading, respectively. Inset is a close-up of the SARS-CoV PL^{pro} (left panel) and HAUSP (right panel) active sites. Backbone atoms are shown as ribbons, and active-site residues are shown as sticks. The BL2 loop is indicated with an arrow. (B) Crystal structure of the SARS-CoV Lys48-linked diUb complex (PDB ID: **5E6J**). SARS-CoV PL^{pro} is shown in red, bound to Lys48-linked diUb, shown as a slate cartoon with transparent surface. Inset is a close-up on the hydrophobic interactions occurring between PL^{pro} and the distal domain of Lys48-linked diUb, with relevant residues shown as sticks. (C) Crystal structure of the MERS-CoV PL^{pro} domain in complex with Ub (PDB ID: **4RF0**). MERS-CoV PL^{pro} is depicted in green cartoon, and Ub is shown in orange cartoon with transparent surface. Dotted box depicts a close-up of the interaction between MERS-CoV PL^{pro} residue Val1691 and Ub residue Ile44, with residues depicted as sticks.

selective disruption. To achieve this, we determined the crystal structure of PL^{pro} covalently bound to Ub, providing a clear picture of the PL^{pro}–Ub interface (Fig. 5C) [162]. Specifically, mutation Val1691Arg was found to significantly disrupt the interaction between PL^{pro} and the hydrophobic Ile44 patch of Ub by introducing a repulsive charge and steric bulk at a key position on the S1 Ub-binding site of PL^{pro} (Fig. 5C). This mutation, along with others, abrogated DUB activity yet permitted polyprotein cleavage at the nsp2–3 junction, thus providing an ideal system to directly assess whether PL^{pro} DUB activity alone disrupts cellular signaling. PL^{pro} inhibited MAVS- and IRF3-mediated IFN-β promoter activity, while DUB-deficient PL^{pro} was unable to interfere, implicating the DUB activity of PL^{pro} directly in the evasion of cellular signaling pathways involved in innate immunity [162]. While this immune evasive activity had been previously noted [157,158,163], it had not been directly linked to the DUB function of PL^{pro}. Additionally, PL^{pro} has been found to interfere with the production of pro-inflammatory cytokines [163]. Interestingly, Yang and coworkers observed that PL^{pro} active-site knockout mutants also prevented ubiquitination in cell culture, suggesting a protease-independent inhibition of Ub conjugation, although this has not been confirmed by others [157]. Importantly, selective interference of PL^{pro} DUB activity could enable future engineering of replication-competent, DUB-deficient MERS-CoV that could be used to investigate the role of PL^{pro} DUB activity during MERS-CoV infection.

Not surprisingly, MERS-CoV PL^{pro} has been identified as a target for small-molecule drug design [159,165,166], but the development of MERS-CoV-specific antiviral compounds remains in its early stages. Phage display methods have been successful in identifying inhibitors of Ub-binding proteins through the generation of Ub variants (UbVs) with significantly enhanced affinity toward their cognate Ub-binding partners, providing a novel and promising platform for the development of Ub-based therapeutics [167–170]. Recently, UbVs have been identified that potently and selectively inhibit the DUB, deISGylating, and polyprotein processing activities of MERS-CoV PL^{pro}. Furthermore, expression of the UbVs in MERS-CoV-infected cells resulted in a 4-log reduction in infectious viral progeny [171], demonstrating the promising potential for virus-specific therapies developed using Ub phage display methods.

HCoVNL63 PLP2

HCoV-NL63 possesses two PLP domains, PLP1 and PLP2. PLP2 cleaves the viral polyprotein to release nsp2 and nsp3, although it does not cleave following a diGly motif as found for other CoV PLPs; instead, it has been reported to recognize FTKLAG↓GK and VAKQGA↓GF sites within the viral polyprotein [172]. Nevertheless, NL63 PLP2 also possesses DUB activity, cleaving Lys48-linked [172] and Lys63-linked polyUb chains [138], and ISG15 [173]. Initial work demonstrated that HCoV-NL63 infection resulted in impaired IFN-β secretion in cell culture [138], and subsequent studies investigated the role of PLP2 in downregulating the cellular innate immune response. PLP2 downregulated Sendai virus- and RIG-I-mediated IFN-β promoter activity [133], and Poly-I:C-induced, TLR3-dependent IFN-β promoter activity [138]. Consistent with these observations, PLP2 deubiquitinated RIG-I, TBK1, IRF3, and STING in overexpression experiments [174]. Its role in downregulating TNF-α-induced, NF-κB-dependent signaling pathways was also suggested [133]. Interestingly, PLP2 also appears to downregulate RIG-I-mediated IFN-β production irrespective of its catalytic activity [138].

MHV PLP2

Sequencing ORF1a and ORF1b of MHV strain JHM identified, besides the main protease, two putative cysteine protease domains, PLP1 and PLP2, which shared homology with cellular PLPs around the putative catalytic Cys and His residues [175]. The autoproteolytic activity of PLP2 toward the MHV polyprotein was later demonstrated [176], and the cleavage site within the viral polyprotein recognized by PLP2 was determined to be FSLKGG↓AV. DUB activity of MHV PLP2 was predicted based on the conservation of its active-site residues with the SARS-CoV PL^{pro} domain and later confirmed *in vitro*, displaying efficient activity toward Lys11, Lys48, and Lys63 diUb and human ISG15 [177]. MHV PLP2 was found to inhibit cellular transcription of IFN-β *via* RIG-I, MAVS-, TBK1-, and IRF3-mediated induction pathways [133,178] and inhibition of IRF3 phosphorylation and nuclear translocation [179]. Further investigation into the mechanism of IRF3-specific inhibition of IFN-β production suggested that TBK1 and, curiously, IRF3 were directly deubiquitinated by PLP2 [178,179]. The crystal structure of MHV PLP2 was eventually determined and revealed a Cys-His-Asp catalytic triad, with a Gln residue as a putative contributor to the oxyanion hole, in contrast to the Trp residue found in SARS-CoV PL^{pro} [135]. Significant structural homology was observed with respect to other CoV PLP2/PL^{pro} domains, with MHV PLP2 adopting the thumb, palm, and fingers domain architecture common to USP DUBs. Interestingly, mutations in the UBL domain adjacent to MHV PLP2 impaired DUB activity and reduced the thermostability of PLP2 [180].

Additional CoV PLPs

TGEV and PEDV both encode two PLP domains, named $PL1^{pro}$/$PL2^{pro}$ and PLP1/PLP2, respectively.

TGEV PL1^{pro} resides in nsp3, cleaving the viral polyprotein at a single site at the nsp2–3 junction following a diGly motif [181], and it was shown to possess DUB activity toward Lys48- and Lys63-linked polyUb chains *in vitro* [182]. A crystal structure of TGEV PL1pro revealed that it possesses the palm, thumb, and fingers subdomain typical of other viral PL^{pro} and eukaryotic USP domains [182]. In terms of the active-site construction of the enzyme, a Cys-His-Asp catalytic triad observed at the interface between the thumb and palm and a glutamine was found to be a likely contributor to the oxyanion hole, occupying a spatially homologous position to that of Trp107 found in the SARS-CoV PL^{pro} domain. A notable difference from other PLPs was the absence of an N-terminal UBL domain, which is only conserved in the region preceding the second PLP domain in CoVs.

The PLP2 domain from PEDV has also been confirmed to deubiquitinate cellular proteins in cell culture and interfere with host innate immune signaling pathways, although its role in polyprotein processing remains to be characterized [183]. PEDV PLP2 inhibited RIG-I-mediated IFN-β expression and NF-κB-responsive promoter activity, although to a lesser extent than HCoV-NL63 PLP2 [183]. Inhibition of STING-mediated IFN-β expression was also observed [183].

The avian infectious bronchitis virus (IBV), a prototypical member of the CoV family, had a single PLP (PL^{pro}) identified at the 5′ end of its genome, based on the conservation of catalytic Cys and His residues with cellular PLPs and two MHV PLPs [175]. IBV PL^{pro} was found to cleave the polyprotein between Gly–Gly residues at two sites, releasing nsp2 and nsp3 [184–187]. It adopts a fold common to USP DUBs and possesses an N-terminal UBL domain seen in most other CoV PL^{pro} domains [188], and it cleaves Lys48- and Lys63-linked polyUb chains [189], with an apparent preference for Lys63 linkages [188]. While DUB activity of IBV PL^{pro} has been demonstrated, the importance of this function has not been established.

Arteriviridae

In addition to CoV, the Nidovirales order includes the Roniviridae, Mesoniviridae, and Arteriviridae families that contain viruses with smaller positive-sense ssRNA genomes relative to the CoV, with sizes of roughly 26, 20, and 15 kb, respectively [190]. The arterivirus family currently consists of four virus species that each infect a specific non-human mammal causing persistent infection or acute disease associated with abortions, respiratory disease, or lethal hemorrhagic fever [191]. Equine arteritis virus (EAV) and especially porcine reproductive and respiratory syndrome virus (PRRSV) have a tremendous economic impact on the veterinary industry worldwide [192,193]. The two other arteriviruses are simian hemorrhagic fever virus (SHFV) and lactate dehydrogenase-elevating virus (LDV), the latter infecting mice. Arteriviruses have a number of features that are similar to CoVs such as virion composition, genome structure, and some of the replicase polyprotein functions and their replication strategy. The expression of nsps from large polyproteins is also similar to what was described for CoVs (see former paragraph). The arterivirus polyproteins are cleaved into individual nsps by internally encoded PLPs located in nsp1 and nsp2 to release nsp1 and nsp2, respectively, and a 3CLpro in nsp4 that cleaves all junctions downstream of nsp3. While EAV nsp1 contains a single active protease named PLP1, PRRSV and LDV nsp1 contain two protease domains each: PLP1α and PLP1β. In the case of SHFV, there are three functional PLPs in nsp1 that release nsp1α, β, and γ [191,194]. The PLP2 protease in nsp2 of arteriviruses was shown to cleave the nsp2–3 junction [195]. Similar to EAV and PRRSV PLP2, as further elaborated below, SHFV and LDV PLP2 were shown to additionally possess DUB activity and limit innate immune activation by removing Ub from overexpressed RIG-I [196].

EAV PLP2

The nsp2 protease has been suggested to belong to a novel OTU-like superfamily of cysteine proteases [197], strengthened by the evidence that conserved Cys and His residues are required for its protease activity [195]. After several human OTU domain proteins were identified and shown to have DUB activity, the Ub-deconjugation activity of a number of viral OTU domains, including EAV PLP2, was examined [198]. Ectopic expression of the PLP2 domain alone, or full-length EAV nsp2, indeed resulted in decreased global levels of both Ub and ISG15 conjugates in cultured cells. Genuine DUB activity of EAV PLP2 on both Lys48- and Lys63-linked polyUb chains was further confirmed by *in vitro* assays using purified protein [196]. EAV PLP2 was therefore concluded to have dual activity toward the viral replicase polyproteins and Ub(-like) conjugates. Interestingly, cellular OTU domain-containing DUBs generally seem much less promiscuous, as they do not cleave ISG15 conjugates [198] and are usually at least partly specific for certain Ub linkages [19]. NF-κB activation by TNF-α was suppressed upon the expression of EAV PLP2 [198], hinting at an innate immune suppressive function of the vDUB. EAV PLP2 also inhibits RIG-I-mediated innate immune signaling upon overexpression and is able to deubiquitinate RIG-I [196].

A crystal structure of EAV PLP2 bound to Ub revealed a remarkably compact OTU fold, including a C4 zinc finger not previously observed in OTU

domains and an active site consisting of the conserved Cys and His residues (Fig. 6) [199]. Interestingly, PLP2 bound Ub in an orientation comparable to that of a viral OTU domain Crimean-Congo hemorrhagic fever virus (CCHFV; see below), with the zinc finger domain performing an analogous role in orienting Ub binding as a β-hairpin present in the CCHFV OTU domain, which appears to assist in expanding the substrate specificity of PLP2 to include ISG15, as was observed for the CCHFV enzyme [200]. Guided by the structure (Fig. 6), we mutated the Ub-binding surface on PLP2 to prevent Ub binding while leaving the active site of the protease unperturbed [199]. Indeed, recombinant EAV virus containing these mutations displayed wild-type replication kinetics in cell culture infections, confirming that polyprotein processing by PLP2 was unaffected. Primary equine lung fibroblasts were then infected with the DUB-negative viruses and compared to wild-type EAV. Significantly enhanced innate immune responses were measured in the mutant virus infections (by comparing mRNA levels of IFN-β, MX1, and IL8), which provided direct evidence that vDUB activity supresses host antiviral responses. This opens the possibility of using DUB-negative viruses that display reduced innate immune suppressive activity (with respect to wild-type virus) as next-generation attenuated live virus vaccines. A vaccination challenge trial in horses comparing wild-type and DUB-negative EAV resulted in slightly decreased replication of the DUB-negative virus but comparable clinical disease, antibody response, and innate immune response [201]. It should be noted that under the experimental conditions, no difference was measured between the two viruses, which might be explained by the already high level of protection induced by the wild-type virus [201].

Interestingly, despite the fact that arteriviruses and CoVs are members of the same order of Nidoviridae, suggesting a relatively close evolutionary connection, arteriviruses encode an OTU-like DUB, while CoVs encode a USP DUB. This suggests that the virus families each independently acquired DUBs into their genomes, again emphasizing the apparent importance of such activity for these viruses.

PRRSV PLP2

PRRSV PLP2 possesses both in *trans* and in *cis* cleavage activities, and mutations disrupting only *trans*-cleavage activity were lethal for the virus [202]. Probing the nsp2/3 cleavage site revealed that the cleavage site is at the Gly1198 + 1199 dipeptide [202]. Besides full-length nps2, many different isoforms of nsp2 having the same N terminus were detected during infection in cell culture [203]. These likely at least partly account for cleavage products of nsp2 when other conserved Gly dipeptide sites are processed by PLP2. More recently, two nsp2 products were identified as a result of −2 and −1 ribosomal frameshifting in the nsp2 region of the polyprotein gene, yielding nsp2 trans frame (TF) and nsp2N products, respectively [204]. Nsp2TF contains a different C-terminal transmembrane domain compared to nsp2 and localized to different intracellular compartments. Removal of nsp2TF attenuated the virus as it replicated slower than wild-type virus and reached lower peak titers [204]. For this frameshift event, the frameshift site, a frameshift-stimulatory

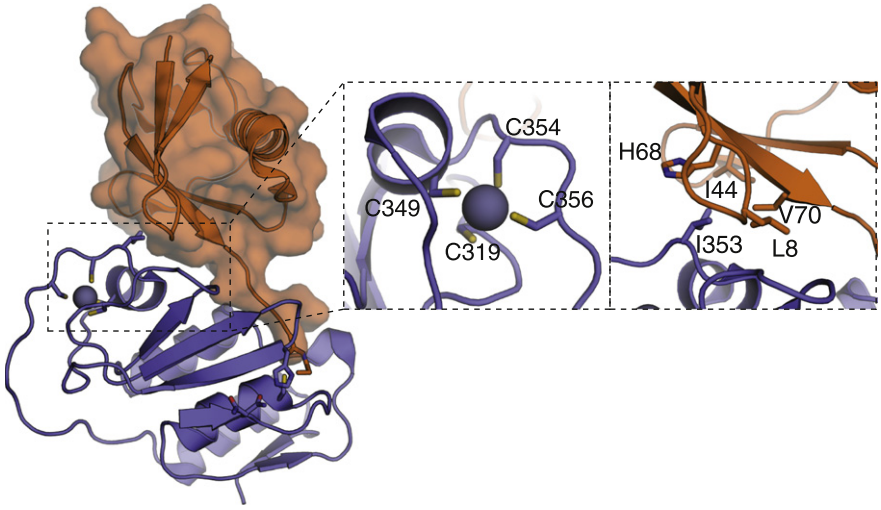

Fig. 6. Crystal structure of the EAV PLP2–Ub complex. EAV PLP2 (PDB ID: **4IUM**) is shown in slate, covalently bound to Ub (orange, transparent surface). Depicted inset is the 4C Zn finger (left panel), with Zn-coordinating residues shown as sticks and Zn shown as a gray sphere. EAV PLP2 residue Ile353 forms hydrophobic interactions with the indicated residues on Ub (inset, right panel), and targeted disruption of Ile353-mediated interactions selectively abrogated PLP2 DUB activity.

element, and, uniquely, a protein factor, nsp1β, are required [205]. Some of the nsp2 isoforms were found to be present in or on virus particles and might participate in entry, early steps of virus replication, or suppression of host immune responses [206].

PRRSV PLP2 was shown to possess DUB activity toward Ub and ISG15 conjugates [198,207]. PLP2 inhibited NF-κB activation in overexpression experiments by interfering with the Lys48-linked polyubiquitination of IκBα and thereby preventing its degradation [208]. RIG-I was also deubiquitinated upon overexpression of PRRSV PLP2, suggesting that the DUB activity of PLP2 is responsible for evading RIG-I-induced innate immune responses [196]. PLP2 of JXwn06, a highly pathogenic PRRSV strain, and that of a modified live virus vaccine strain, were shown to cleave all diUb chains linked through the different Lys in Ub, but not linear diUb *in vitro* [209]. The greatest difference between these PLP2s was that JXwn06 was more active toward Lys63-linked diUb than modified live virus. *In vitro*, PLP2 cleaved neither human ISG15-7-amino-4-methylcoumarin (ISG15-AMC) nor the pro-forms of human ISG15 or porcine ISG15, which contradicts the earlier observation of ISG15 conjugate cleavage upon ectopic expression of PLP2 [198,207,209]. With respect to the different isoforms of PPRSV nsp2 that include PLP2, no studies have been carried out to assess the specific DUB activities of these variants and their functional contribution during infection.

Nairoviruses

Nairoviruses are enveloped, negative-sense ssRNA viruses within the family *Bunyaviridae*, which can be further subdivided into serogroups based on antibody cross-reactivities. The serogroups discussed here include the Crimean-Congo haemorhaggic fever serogroup, which includes CCHFV; the Nairobi sheep disease serogroup, which includes the Nairobi sheep disease virus (NSDV) and Dugbe virus (DUGV); and the Thiafora serogroup, which includes the Erve virus (ERVV). Nairovirus genomes share a similar structure and are composed of three ssRNA segments, small (S), medium (M), and large (L), named as such for their respective nucleotide lengths.

CCHFV is a widespread tick-borne virus that is transmitted to humans primarily by members of the *Hyalomma* genus [210]. Infection with CCHFV can lead to hemorrhaging and multi-organ failure, with a case fatality rate ranging from 10 to 40%. Currently, there is no protective vaccine, and treatment involves only basic management of CCHF symptoms. Contrary to CCHFV, DUGV infection does not lead to serious disease in humans and is instead associated with mild febrile illness. In contrast, ERVV infections have been postulated to cause "thunderclap headaches" in humans [211], with mice and shrews suspected as potential reservoirs for the virus [212].

CCHFV OTU

In 2000, Makarova and coworkers published the discovery of a novel cysteine protease superfamily, based on sequence homology with the *Drosophila* OTU gene product [197]. While an OTU domain was initially identified at the N terminus of the DUGV L protein, sequence determination of the CCHFV L-segment later uncovered the presence of a homologous nairovirus OTU domain [213,214].

Following the discovery that A20, a cellular protein with an OTU domain that negatively regulates NF-κB signaling *via* deubiquitination [215,216], Frias-Staheli and coworkers investigated the role of viral OTU domains *in vivo* and demonstrated that the CCHFV OTU domain indeed possessed DUB activity, actively processing Lys48 and Lys63 polyUb chains and ISG15 *in vitro* and globally deconjugating Ub and ISG15 from cellular proteins during ectopic expression [198]. Expression of the CCHFV OTU domain diminished activity at an NF-κB-responsive promoter during TNF-α stimulation and established the CCHFV OTU domain as a viral protease involved in the evasion of the cellular innate immune response. The work culminated with the description of a chimeric Sindbis virus expressing the CCHFV OTU domain along with ISG15, which was found to increase lethality in IFN-αβ receptor$^{-/-}$ background mice, effectively preventing ISG15-mediated protection of Sindbis virus lethality. Following work demonstrated that the CCHFV OTU domain mitigates RIG-I-mediated IFN-β expression, suggesting that the enzyme inhibits both antiviral and pro-inflammatory branches of the innate immune response during infection [196].

Crystal structures of the CCHFV OTU domain were subsequently reported bound to Ub [217–219], full-length ISG15 [217], or the C-terminal β-grasp domain of ISG15 [218], and in its *apo* form [218] and together provided the first structural insights into a viral OTU protease. The CCHFV OTU domain was found to contain α-helical and β-sheet lobes [217,218] and closely resembled the structure of the eukaryotic OTU-domain-containing protein from yeast (yOTU1) (Fig. 7A) [220]. The active site of CCHFV OTU was composed of a Cys-His-Asp catalytic triad, arranged in catalytically competent geometry in all reported structures [217,218], and while no side chains were suitably oriented to participate in the formation of the oxyanion hole, the backbone amides of the catalytic Cys40 and a nearby Asp37 were proposed to serve this function [217].

Interestingly, while Ub and ISG15 bound to CCHFV OTU in similar orientations (Fig. 7A and B), the β-grasp domains of these substrates were rotated ~75° with respect to the orientation that Ub binds to a

representative eukaryotic OTU DUB from yeast, yOTU1 (Fig. 7A). Interestingly, the alternate binding orientation of Ub and ISG15 to the CCHFV OTU was due, in part, to the presence of a unique β-hairpin that forms a substantial part of the substrate binding surface on the viral enzyme (Fig. 7A). The β-hairpin structure was thus proposed to facilitate a rotated binding orientation for Ub that also accommodated basic residues within the C-terminal β-grasp domain of ISG15, which appear to prevent its interaction with the yOTU1 [217]. Using structure-guided mutagenesis, the DUB and deISGylating activities of CCHFV OTU could be decoupled by exploiting unique interactions between the OTU domain and its cognate substrates, targeting a helical arm structure conserved in most OTU domains in order to disrupt deISGylating activity and a unique hydrogen bonding interaction occurring at the interface of Ub and the novel β-hairpin structure of CCHFV OTU [218].

In vitro works by multiple groups have shown that CCHFV OTU is active toward Lys6, Lys11, Lys48, and Lys63 Ub chains [218,221]. It was also demonstrated that CCHFV OTU cleaves fluorogenic Ub-AMC and ISG15-AMC substrates, with some groups observing a preference for the Ub substrate [218,219,221], and others demonstrating similar activities toward both substrates [217]. Furthermore, Akutsu and coworkers saw a marked increase in activity toward a fluorescent Lys63-linked diUb substrate compared to Lys48-linked diUb, providing kinetic evidence for CCHFV OTU linkage specificity [218]. While this demonstrates that CCHFV OTU may be somewhat capable of discriminating between Ub linkage types, structural evidence is necessary to confirm the molecular basis for the observed specificities. Recent advancements in CCHFV reverse genetics systems [222] may also soon enable studies that directly reveal the role of the DUB and deISGylating activities of the OTU domain during CCHFV infection.

DUGV OTU

Similar to the CCHFV OTU domain, the DUGV OTU domain was found to be an effective DUB and deISGylase removing Ub and mISG15 in cell culture [198,223] and also a potent DUB *in vitro* cleaving Lys6-, Lys11-, Lys48-, and Lys63-linked diUb and Lys6 linkages with particular efficiency [221]. It was also demonstrated that the DUGV OTU was ineffective at processing ISG15, and a description of the DUGV OTU crystal structure in complex with Ub and a comparison with CCHFV OTU suggested that the inability of DUGV OTU to process ISG15 was centralized around residue Thr128, which was unable to form a hydrogen-bonding network with ISG15 comparable to the CCHFV OTU residue Glu128. The introduction of Glu128 to DUGV OTU indeed increased reactivity toward a fluorogenic ISG15 substrate by 2000% [221]. Additional

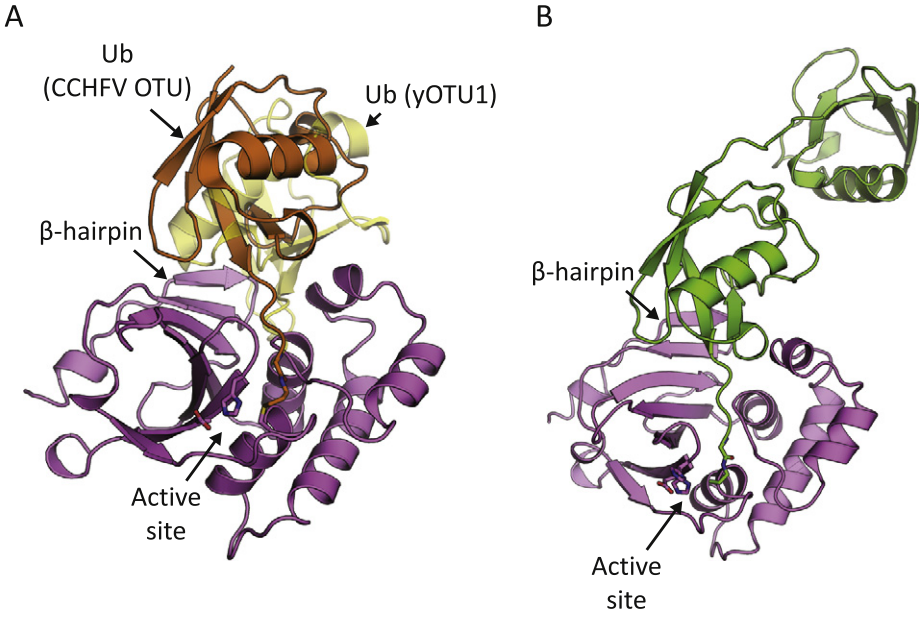

Fig. 7. CCHFV OTU interacts with Ub and ISG15 in a rotated orientation with respect to yOTU1. (A) Comparison of the Ub-binding orientations of the CCHFV OTU and yeast OTU1 OTU (yOTU1) domains. CCHFV OTU (PDB ID: **3PT2**; violet) is shown bound to Ub (PDB ID: **3PT2**; orange), and the β-hairpin is indicated with an arrow. yOTU1 in complex with Ub (PDB ID: **3BY4**) was superposed onto the CCHFV OTU structure, and yOTU1 was removed for clarity. The yOTU1-bound Ub domain is shown in transparent yellow. (B) Crystal structure of CCHFV OTU (PDB ID: **3PSE**; purple) in complex with ISG15 (PDB ID: **3PSE**; green). CCHFV OTU binds ISG15 in a comparable orientation to Ub.

similarities with the CCHFV OTU domain were found in its ability to downregulate cellular immune response pathways, where both NF-κB- and IFN-responsive promoter activities were disabled upon stimulation in the presence of DUGV OTU [223].

ERVV OTU

In contrast to CCHFV and DUGV OTU domains, the ERVV OTU domain is essentially free of DUB activity, possessing only activity against ISG15, with a particularly high affinity for human ISG15 as determined by isothermal titration calorimetry [221,224]. Analysis of a crystal structure of ERVV OTU in complex with mISG15 attributed the inability of ERVV OTU to bind Ub to the presence of an electrophilic region (Arg21, Ser132, Asn134) at the interface that binds ISG15, which appears to be able to accommodate ISG15 residue Glu87, but not the spatially conserved hydrophobic Ub residue Leu8 [224].

NSDV OTU

Transfection of Vero cells with NSDV OTU was found to reduce activity at the IFN-β and IFN-responsive promoters in a protease-dependent fashion, demonstrating that NSDV OTU interferes with both the production and activity of IFN [225]. Furthermore, NSDV OTU was shown to deubiquitinate and deISGylate cellular proteins during expression, thus establishing it as a DUB capable of interfering with the production and activity of IFN [225].

Picornaviridae

Picornaviruses are small, non-enveloped positive-sense ssRNA viruses. Within the family *Picornaviridae*, several viruses are known to cause disease in livestock, and indeed, the foot-and-mouth disease virus (FMDV) was the first discovered animal virus [260]. A member of the *Aphthovirus* genus, FMDV, remains an economically significant pathogen in the livestock industry. FMDV infection is characterized by the formation of vesicles on the feet and mouths of infected animals and can lead to substantial economic losses annually due to decreased animal productivity and trade restrictions imposed on infected livestock. Certain members of the *Enterovirus* genus within the family *Picornaviridae* also cause disease in livestock, and recently, an isolate of porcine *Enterovirus* species G (EVG) was identified that contained a Torovirus PLP domain that appears to have been acquired through cross-order recombination [226].

FMDV L^{pro}

Early research on FMDV identified a cleavage product originating from the N terminus of the viral polyprotein [227]. The cleavage was initially proposed to result from a host protease but was later found to be carried out autoproteolytically by an FMDV-encoded leader protease (L^{pro}) located within the N terminus of the nascent polyprotein [228]. Translation of L^{pro} can initiate at one of the two in-frame start codons, leading to the production of Lab^{pro} and Lb^{pro} isoforms, the former having an additional 28 aa at the N terminus.

Prior studies identified L^{pro} as a potential virulence factor, with L^{pro} cleaving the host eukaryotic translation initiation factor 4 gamma (eIF4G) that is involved in the translation of cellular and capped mRNA transcripts, thereby prioritizing the translation of viral transcripts [229]. Experiments using an FMDV mutant lacking the L^{pro} domain also implicated the protease in the circumvention of cellular innate immune responses by the inhibition of cellular IFN-α/β production and associated ISGs, specifically protein kinase R, a cytoplasmic sensor of viral RNA [230–234]. In an attempt to disrupt this activity, de Los Santos *et al*. generated an FMDV virus with point mutations Ile83Ala and Leu86Ala within L^{pro}, and as predicted, these mutations attenuated viral replication, with infection resulting in an increased cellular IFN-β expression [235]. Notably, the autoprocessing activity of the FMDV L^{pro} mutant was unaffected, as was its ability to cleave eIF4G [235].

Early bioinformatics results predicted L^{pro} to be a PLP [236,237], sharing sequence similarity with MHV PLPs near the putative catalytic Cys [238]. This was later confirmed upon determination of the Lb^{pro} crystal structure, which also provided insight into the autocatalytic mechanism of Lb^{pro} [237], and, in fact, represents the first structural characterization of a viral papain-like cysteine protease [237]. The C-terminal polyprotein cleavage site recognized by Lb^{pro} was present in the crystallized construct and found to occupy the active site of an adjacent Lb^{pro} monomer, mimicking a product-bound complex (Fig. 8). While this *trans* interaction may suggest that Lb^{pro} removal also occurs in *trans* within the context of polyprotein maturation, the authors proposed that the removal of Lb^{pro} may also occur in *cis*, due in part to the relatively weak intermolecular contacts between Lb^{pro} monomers and the propensity for the residues within extended C terminus of Lb^{pro} to turn over the protease into the active-site cleft. NMR results, however, show that Lb^{pro} exists as a homodimer in solution [239].

Wang *et al*. further investigated the structure of Lb^{pro}, and using secondary-structure matching discovered that it shared structural homology with SARS-CoV PL^{pro} and the eukaryotic USP14, two previously characterized DUBs, which lead to the hypothesis that L^{pro} may also possess DUB activity [240]. This was confirmed *in vitro*, where L^{pro} cleaved Lys48- and Lys63-linked polyUb chains and globally deubiquitinated cellular proteins during ectopic expression [240]. Based on previous findings that

the IFN antagonist and eIF4G processing functions of L^{pro} were apparently independent [235], Wang and coworkers sought to determine if the DUB and eIF4G processing activities were similarly uncoupled. Indeed, the previously characterized Ile83Ala/Leu86Ala L^{pro} mutant was deficient in DUB and IFN-supressing activities yet retained the ability to hydrolyze eIFG4, effectively linking the DUB and immunosuppressive properties of L^{pro} [240]. Furthermore, overexpression of L^{pro} resulted in a reduction of Ub-conjugated RIG-I, TBK1, TRAF3, and TRAF6, providing evidence for the role of L^{pro} in supressing host Ub-dependent innate immune signaling pathways *via* deubiquitination of cellular signaling components [240].

While a considerable amount of work has gone into the structural and functional characterization of L^{pro}, a number of questions remain. While the autocatalytic activity and substrate specificity of L^{pro} have been characterized, which have led to the development of peptidomimetic compounds as potential inhibitors of L^{pro} [241–243], the molecular basis for Ub recognition by L^{pro} remains to be elucidated. Mutagenesis has been able to discriminate between the DUB activity and polyprotein/eIFG4 processing activities of L^{pro}; however, it is still unclear how these mutations exert their selective effect. It is interesting to note that Ile83Ala/Leu86Ala mutations targeted the SAF-A/B, Acinus, and PIAS (SAP) domain within L^{pro} [235], and while these mutations selectively abrogate DUB activity [240] and delay nuclear translocation [235], they do not appear to target the likely Ub-binding interface of L^{pro}, which has been demonstrated to be an effective means to inhibit the DUB activity of other vDUBs [162,199]. Further adding to the complexity of its role in innate immune suppression, L^{pro} has been implicated in the degradation of NF-κB, although this activity has not been demonstrated directly [234]. The structural characterization of L^{pro} in complex with Ub should shed light on some of these questions.

EVG ToV-PLP

Recently, an EVG isolate was identified containing a previously unseen insertion between non-structural proteins 2C and 3A, flanked by $3C^{pro}$ cleavage sites [226]. Further analysis determined that the inserted sequence shared significant similarity with the Torovirus (a member of the order *Nidovirales*) nsp3-like PLP at the amino acid level, which was subsequently termed ToV-PLP. Homology modeling predicted structural similarities between ToV-PLP and the FMDV L^{pro}, leading to the hypothesis that ToV-PLP may possess DUB/deISGylating activities. These suspicions were confirmed, with ToV-PLP showing global DUB and deISGylating activity in cell culture and *in vitro* analysis demonstrating that ToV-PLP processed ISG15, Lys48-, and Lys63-linked polyUb chains and curiously showed activity toward Met1 linear Ub chains [226]. Infection of swine testicular cells with recombinant EVG lacking ToV-PLP increased cellular type I and type II IFN production and ISG15 transcription and displayed impaired growth kinetics compared to its ToV-PLP-containing counterpart [226]. Although *Enteroviruses* are known to have high rates of genetic recombination, the cross-order acquisition of a novel DUB by EVG is likely a rare event [226], and the apparent increase in viral fitness with respect to DUB-negative EVG further demonstrates the importance of vDUBs in supressing the innate immune response of their hosts.

Tymoviridae

The turnip yellow mosaic virus (TYMV) is the type species of the family *Tymoviridae*, a group of positive-sense ssRNA viruses infecting plants. Their non-structural proteins are expressed from two overlapping ORFs, ORF-206 and ORF-69 [244], which encode for p206 and p69, respectively. The TYMV PLP (PRO) domain is encoded within ORF-206 and cleaves the

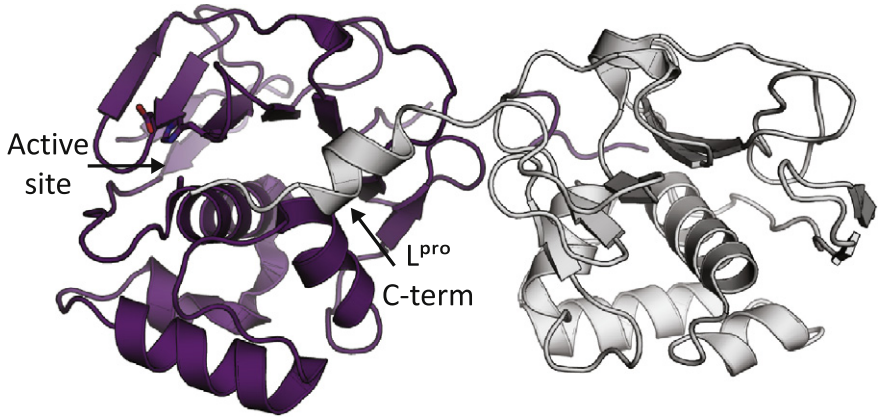

Fig. 8. Crystal structure of FMDV Lb^{pro}. FMDV Lb^{pro} (PDB ID: **1QOL**) is shown in cartoon, and an adjacent monomer in the asymmetric unit is depicted in gray, with the C terminus leading toward the active site of the adjacent Lb^{pro} monomer.

translation product, p206, at two sites releasing p98, p42, and p66 [245–248]. During infection by the virus, the host actively supresses accumulation of the TYMV RNA-dependent RNA polymerase domain (POL), located in p66, by tagging it with Lys48-linked polyUb, targeting it to the Ub-proteasome system [249]. Appreciating that the TYMV PRO consensus site (K/R)LX(G/A/S)(G/A/S) [248] was compatible with the C terminus of Ub, Chenon *et al*. suggested that PRO may counter this cellular defence mechanism by stabilizing the POL domain during infection *via* removal of the Lys48-Ub chains [250]. Indeed, PRO is able to process Lys48- and Lys63-polyUb chains *in vitro*, and pulse-chase analysis determined that expression of PRO stabilized p66 in a protease-dependent manner [250].

Hidden Markov model comparison predicted that TYMV PRO shared secondary structure elements with a number of eukaryotic and viral OTU domains, and sequence similarities were identified surrounding the catalytic Cys and His residues, in agreement with the characterized OTU domain [197,250]. The crystal structure of the TYMV PRO domain revealed a compact protease domain, composed of α-helical and β-sheet lobes, which hosted the catalytic Cys and His residues, respectively, and a unique N-terminal lobe (Fig. 9) [251]. A structural comparison using the DALI alignment server also detected significant structural similarities with previously reported viral and eukaryotic OTU domains, placing the TYMV PRO domain within the OTU superfamily [200]. In general, the active site of PLPs is canopied by a loop structure. The active site of PRO possesses no such loop, making its active site entirely solvent exposed [251]. Also absent was the third residue thought to align the histidine imidazole ring for proper catalysis. Taken together, the pared-down, solvent-exposed active site of PRO was thought to account for its relatively poor DUB activity in comparison to other OTU DUBs and the relaxed specificity of the enzyme at the P1 site [251]. Structural evidence for the in *trans* cleavage activity of PRO was also revealed, with the C terminus of one PRO domain bound into the cleft leading toward the active site of a nearby symmetry mate (Fig. 9) [251]. Based on this structure, the strict requirements at P5 and P4 were rationalized by the presence of complementary acidic and hydrophobic pockets, respectively, on the surface of PRO [251]. Further *in silico* docking studies predicted that the N-terminal lobe of PRO interacts with the hydrophobic Ile44 patch of Ub [251].

Concluding Remarks

Significant effort has been dedicated to uncovering the cellular substrates and structural biology of vDUBs, and the role of these enzymes during infection is now beginning to emerge. However, more work is needed is clarify the picture, since many experiments used to ascertain the cellular targets of vDUBs have relied on overexpression experiments and thus may not accurately reflect the circumstances of an actual viral infection. Both the cellular ubiquitination system and viral protein expression are dynamic processes, with the temporal and spatial regulation of these events likely playing a significant role in determining which substrates are accessible to a given vDUB. To complicate matters further, vDUB domains often exist within larger multidomain proteins, some of which are membrane bound, yet they are often studied in isolation as soluble cytoplasmic proteins in cell culture, likely unable to exhibit subcellular localization patterns, which would be found under biologically relevant conditions. Moreover, additional viral factors present during infection may influence the substrate specificity of a vDUB in question. Indeed, emerging technologies are addressing some of the challenges in accurately analyzing Ub-dependent signaling pathways, with powerful mass spectrometry and proteomics methods targeted at probing the dynamics of these systems, including the stoichiometry and kinetics of Ub conjugation, and the specific linkage types populating cellular substrates of interest (reviewed in Ref. [252]). These technologies could now be directed toward revealing the cellular targets and linkage specificities of vDUBs during the course of live virus infection. Furthermore, it is pertinent to recognize that in cases where a viral protease depends on a single active site for both DUB and proteolytic (i.e., non-isopeptide bond cleavage) activity, a complete understanding of their genuine cellular targets necessitates the selective inhibition of DUB activity, as described for a select number of multifunctional vDUBs [162,199,240].

Protein X-ray crystallography has provided remarkable insights into the molecular basis for how vDUBs recognize and bind monoUb, yet significant questions remain regarding their ability to recognize a particular Ub linkage type. To date, a single example of a vDUB in complex with a diUb substrate has been described [142]; however, exciting new approaches to generate polyUb probes of varying linkage types [253,254] will now undoubtedly enable rapid advances in understanding the structural basis for the recognition of specific linkage types by vDUBs. The recent characterization of several bacterial DUBs has also advanced our understanding of the interplay between the cellular ubiquitination pathways and pathogenic bacteria at a structural level and highlighted key variable regions within bacterial clan CE proteases permitting adaptation to Ub/Ubl domains and specific Ub linkage types [255].

It is now clear that interfering with Ub-dependent cellular processes through deubiquitination is a powerful strategy used by viruses to promote their survival, as evidenced by the large number of DUBs found in diverse virus lineages. While we have made

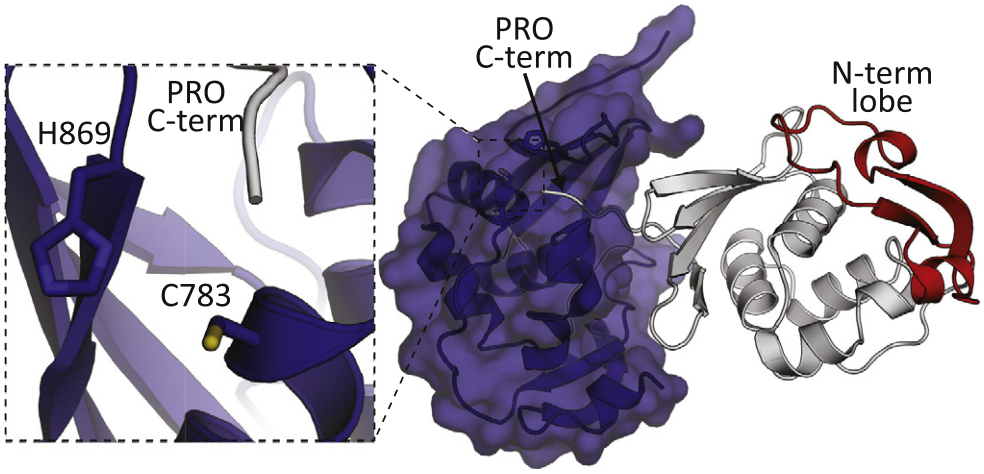

Fig. 9. Crystal structure of TYMV PRO. The TYMV PRO domain (PDB ID: **4A5U**; deep blue, transparent surface) is shown in cartoon. A symmetry mate (gray) is also shown, with the C terminus bound in the active site of the adjacent PRO monomer. The N-terminal lobe is colored red in the adjacent symmetry mate. Dotted box shows a close-up of the pared-down PRO active site, with catalytic residues shown as sticks.

every effort to include all vDUBs that have been described to date, many more undoubtedly remain to be discovered and characterized. Given the growing body of evidence demonstrating the importance of vDUB activity in viral replication and pathogenesis, vDUBs are now recognized as attractive targets for the design of antiviral therapeutics. Small-molecule inhibitors of vDUBs and novel, selective protein-based approaches to disrupt the proteolytic activity of vDUBs are under active investigation, alongside the development of novel live attenuated virus vaccine candidates with impaired DUB activity. Selective targeting of vDUBs by therapeutic intervention or through genetics-based disruption thus holds promising potential for the design of future antivirals and vaccines.

Received 5 May 2017;
Received in revised form 12 June 2017;
Accepted 13 June 2017
Available online 16 June 2017

Keywords:
ubiquitin;
viruses;
papain-like protease;
viral deubiquitinating enzyme;
innate immune evasion

Abbreviations used:
Ub, ubiquitin; UBL, Ub-like; IFN, interferon; ISG, interferon-stimulated gene; ISG15, interferon-stimulated gene 15; DUB, deubiquitinating enzyme; USP, Ub-specific protease; OTU, ovarian tumor protease; PRR, pattern-recognition receptor; TLR, toll-like receptor; RIG-I, retinoic acid-inducible gene I; cGAMP, cyclic-GMP-AMP; cGAS, cyclic-GMP-AMP synthase; MDA5, melanoma differentiation factor 5; MAVS, mitochondrial antiviral signaling protein; TNF, tumor necrosis factor; TRAF, TNF receptor-associated factor; NEMO, NF-κB essential modulator; TANK, TRAF family member-associated activator; TBK1, TANK-binding kinase 1; IRF, IFN regulatory factor; IRF3, IFN regulatory factor 3; STING, stimulator of IFN genes; AdV, adenovirus; HSV-1, herpes simplex virus 1; EBV, Epstein–Barr virus; ORF, open reading frame; MCMV, murine cytomegalovirus; PLP, papain-like protease; RR, ribonucleotide reductase; CRL, Cullin-RING Ub ligase; HCMV, human cytomegalovirus; MDV, Marek's disease virus; KSV, Kaposi's sarcoma virus; CoV, coronavirus; ssRNA, single-stranded RNA; SARS, severe acute respiratory syndrome; SARS-CoV, severe acute respiratory syndrome CoV; MERS, Middle East respiratory syndrome; MERS-CoV, Middle East respiratory syndrome CoV; MHV, mouse hepatitis virus; TGEV, porcine transmissible gastroenteritis; PEDV, porcine epidemic diarrhea virus; nsps, non-structural proteins; HAUSP, herpesvirus-associated USP; BL2, blocking-loop 2; UbV, Ub variant; IBV, avian infectious bronchitis virus; EAV, equine arteritis virus; PRRSV, porcine reproductive and respiratory syndrome virus; SHFV, simian hemorrhagic fever virus; LDV, lactate dehydrogenase-elevating virus; CCHFV, Crimean-Congo hemorrhagic fever virus; AMC, 7-amino-4-methylcoumarin; TF, trans frame; NSDV, Nairobi sheep disease virus; DUGV, Dugbe virus; ERVV, Erve virus; FMDV, foot-and-mouth disease virus; EVG, *Enterovirus* species G; eIF4G, eukaryotic translation initiation factor 4 gamma; TYMV, turnip yellow mosaic virus.

References

[1] D. Komander, M. Rape, The ubiquitin code, Annu. Rev. Biochem. 81 (2012) 203–229.

[2] I. Dikic, S. Wakatsuki, K.J. Walters, Ubiquitin-binding domains—from structures to functions, Nat. Rev. Mol. Cell Biol. 10 (2009) 659–671.
[3] K. Husnjak, I. Dikic, Ubiquitin-binding proteins: decoders of ubiquitin-mediated cellular functions, Annu. Rev. Biochem. 81 (2012) 291–322.
[4] M. Akutsu, I. Dikic, A. Bremm, Ubiquitin chain diversity at a glance, J. Cell Sci. 129 (2016) 875–880.
[5] Y. Kulathu, D. Komander, Atypical ubiquitylation—the unexplored world of polyubiquitin beyond Lys48 and Lys63 linkages, Nat. Rev. Mol. Cell Biol. 13 (2012) 508–523.
[6] R. Yau, M. Rape, The increasing complexity of the ubiquitin code, Nat. Cell Biol. 18 (2016) 579–586.
[7] M.E. Davis, M.U. Gack, Ubiquitination in the antiviral immune response, Virology 479–480 (2015) 52–65.
[8] S.M. Heaton, N.A. Borg, V.M. Dixit, Ubiquitin in the activation and attenuation of innate antiviral immunity, J. Exp. Med. 213 (2016) 1–13.
[9] M. Hochstrasser, Origin and function of ubiquitin-like proteins, Nature 458 (2009) 422–429.
[10] L. Cappadocia, C.D. Lima, Ubiquitin-like protein conjugation: structures, chemistry, and mechanism, Chem. Rev. (2017) http://dx.doi.org/10.1021/acs.chemrev.6b00737.
[11] A.G. van der Veen, H.L. Ploegh, Ubiquitin-like proteins, Annu. Rev. Biochem. 81 (2012) 323–357.
[12] D.J. Morales, D.J. Lenschow, The antiviral activities of ISG15, J. Mol. Biol. 425 (2013) 4995–5008.
[13] M. Hermann, D. Bogunovic, ISG15: in sickness and in health, Trends Immunol. 38 (2017) 79–93.
[14] D. Bogunovic, M. Byun, L.A. Durfee, A. Abhyankar, O. Sanal, D. Mansouri, et al., Mycobacterial disease and impaired IFN-gamma immunity in humans with inherited ISG15 deficiency, Science 337 (2012) 1684–1688.
[15] X. Zhang, D. Bogunovic, B. Payelle-Brogard, V. Francois-Newton, S.D. Speer, C. Yuan, et al., Human intracellular ISG15 prevents interferon-alpha/beta over-amplification and auto-inflammation, Nature 517 (2015) 89–93.
[16] D. Komander, M.J. Clague, S. Urbe, Breaking the chains: structure and function of the deubiquitinases, Nat. Rev. Mol. Cell Biol. 10 (2009) 550–563.
[17] J.M. Fraile, V. Quesada, D. Rodriguez, J.M. Freije, C. Lopez-Otin, Deubiquitinases in cancer: new functions and therapeutic options, Oncogene 31 (2012) 2373–2388.
[18] A.C. Faesen, M.P. Luna-Vargas, P.P. Geurink, M. Clerici, R. Merkx, W.J. van Dijk, et al., The differential modulation of USP activity by internal regulatory domains, interactors and eight ubiquitin chain types, Chem. Biol. 18 (2011) 1550–1561.
[19] T.E. Mevissen, M.K. Hospenthal, P.P. Geurink, P.R. Elliott, M. Akutsu, N. Arnaudo, et al., OTU deubiquitinases reveal mechanisms of linkage specificity and enable ubiquitin chain restriction analysis, Cell 154 (2013) 169–184.
[20] J. Gan, N. Qiao, R. Strahan, C. Zhu, L. Liu, S.C. Verma, et al., Manipulation of ubiquitin/SUMO pathways in human herpesviruses infection, Rev. Med. Virol. 26 (2016) 435–445.
[21] H. Luo, Interplay between the virus and the ubiquitin-proteasome system: molecular mechanism of viral pathogenesis, Curr. Opin. Virol. 17 (2016) 1–10.
[22] P. Wimmer, S. Schreiner, Viral mimicry to usurp ubiquitin and SUMO host pathways, Viruses 7 (2015) 4854–4872.
[23] M.M. Minor, B.L. Slagle, Hepatitis B virus HBx protein interactions with the ubiquitin proteasome system, Viruses 6 (2014) 4683–4702.
[24] V.G. Wilson, The role of ubiquitin and ubiquitin-like modification systems in papillomavirus biology, Viruses 6 (2014) 3584–3611.
[25] A. Calistri, D. Munegato, I. Carli, C. Parolin, G. Palù, The ubiquitin-conjugating system: multiple roles in viral replication and infection, Cell 3 (2014) 386–417.
[26] D. Mattoscio, C.V. Segre, S. Chiocca, Viral manipulation of cellular protein conjugation pathways: the SUMO lesson, World J. Virol. 2 (2013) 79–90.
[27] R.D. Everett, C. Boutell, B.G. Hale, Interplay between viruses and host sumoylation pathways, Nat. Rev. Microbiol. 11 (2013) 400–411.
[28] R. Rajsbaum, A. Garcia-Sastre, Viral evasion mechanisms of early antiviral responses involving regulation of ubiquitin pathways, Trends Microbiol. 21 (2013) 421–429.
[29] K.S. Schulz, K.L. Mossman, Viral evasion strategies in type I IFN signaling—a summary of recent developments, Front. Immunol. 7 (2016) 498.
[30] L.B. Ivashkiv, L.T. Donlin, Regulation of type I interferon responses, Nat. Rev. Immunol. 14 (2014) 36–49.
[31] W.M. Schneider, M.D. Chevillotte, C.M. Rice, Interferon-stimulated genes: a complex web of host defenses, Annu. Rev. Immunol. 32 (2014) 513–545.
[32] S. Smith, C. Jefferies, Role of DNA/RNA sensors and contribution to autoimmunity, Cytokine Growth Factor Rev. 25 (2014) 745–757.
[33] H. Hu, S.C. Sun, Ubiquitin signaling in immune responses, Cell Res. 26 (2016) 457–483.
[34] X. Jiang, Z.J. Chen, The role of ubiquitylation in immune defence and pathogen evasion, Nat. Rev. Immunol. 12 (2011) 35–48.
[35] C. Chiang, M.U. Gack, Post-translational control of intracellular pathogen sensing pathways, Trends Immunol. 38 (2017) 39–52.
[36] K.M. Sparrer, M.U. Gack, Intracellular detection of viral nucleic acids, Curr. Opin. Microbiol. 26 (2015) 1–9.
[37] M.J. McFadden, N.S. Gokhale, S.M. Horner, Protect this house: cytosolic sensing of viruses, Curr. Opin. Virol. 22 (2017) 36–43.
[38] Q. Chen, L. Sun, Z.J. Chen, Regulation and function of the cGAS-STING pathway of cytosolic DNA sensing, Nat. Immunol. 17 (2016) 1142–1149.
[39] R. Rajsbaum, A. Garcia-Sastre, G.A. Versteeg, TRIMmunity: the roles of the TRIM E3-ubiquitin ligase family in innate antiviral immunity, J. Mol. Biol. 426 (2014) 1265–1284.
[40] M.J. May, S. Ghosh, Signal transduction through NF-κB, Immunol. Today 19 (1998) 80–88.
[41] Q. Wang, X. Liu, Y. Cui, Y. Tang, W. Chen, S. Li, et al., The E3 ubiquitin ligase AMFR and INSIG1 bridge the activation of TBK1 kinase by modifying the adaptor STING, Immunity 41 (2014) 919–933.
[42] B.A. Malynn, A. Ma, Ubiquitin makes its mark on immune regulation, Immunity 33 (2010) 843–852.
[43] X. Jiang, L.N. Kinch, C.A. Brautigam, X. Chen, F. Du, N.V. Grishin, et al., Ubiquitin-induced oligomerization of the RNA sensors RIG-I and MDA5 activates antiviral innate immune response, Immunity 36 (2012) 959–973.
[44] S. Reikine, J.B. Nguyen, Y. Modis, Pattern recognition and signaling mechanisms of RIG-I and MDA5, Front. Immunol. 5 (2014) 342.
[45] J. Chen, Z.J. Chen, Regulation of NF-kappaB by ubiquitination, Curr. Opin. Immunol. 25 (2013) 4–12.
[46] S. Chattopadhyay, T. Kuzmanovic, Y. Zhang, J.L. Wetzel, G.C. Sen, Ubiquitination of the transcription factor IRF-3

activates RIPA, the apoptotic pathway that protects mice from viral pathogenesis, Immunity 44 (2016) 1151–1161.
[47] X. Zhao, H. Zhu, J. Yu, H. Li, J. Ge, W. Chen, c-Cbl-mediated ubiquitination of IRF3 negatively regulates IFN-beta production and cellular antiviral response, Cell. Signal. 28 (2016) 1683–1693.
[48] J. Zinngrebe, A. Montinaro, N. Peltzer, H. Walczak, Ubiquitin in the immune system, EMBO Rep. 15 (2014) 28–45.
[49] C.S. Friedman, M.A. O'Donnell, D. Legarda-Addison, A. Ng, W.B. Cardenas, J.S. Yount, et al., The tumour suppressor CYLD is a negative regulator of RIG-I-mediated antiviral response, EMBO Rep. 9 (2008) 930–936.
[50] N. Kayagaki, Q. Phung, S. Chan, R. Chaudhari, C. Quan, K.M. O'Rourke, et al., DUBA: a deubiquitinase that regulates type I interferon production, Science 318 (2007) 1628–1632.
[51] I.E. Wertz, K.M. O'Rourke, H. Zhou, M. Eby, L. Aravind, S. Seshagiri, et al., De-ubiquitination and ubiquitin ligase domains of A20 downregulate NF-kappaB signalling, Nature 430 (2004) 694–699.
[52] A. Ma, B.A. Malynn, A20: linking a complex regulator of ubiquitylation to immunity and human disease, Nat. Rev. Immunol. 12 (2012) 774–785.
[53] K. Parvatiyar, G.N. Barber, E.W. Harhaj, TAX1BP1 and A20 inhibit antiviral signaling by targeting TBK1-IKKi kinases, J. Biol. Chem. 285 (2010) 14,999–145009.
[54] N. Shembade, A. Ma, E.W. Harhaj, Inhibition of NF-kappaB signaling by A20 through disruption of ubiquitin enzyme complexes, Science 327 (2010) 1135–1139.
[55] G. Lopez-Castejon, M.J. Edelmann, Deubiquitinases: novel therapeutic targets in immune surveillance? Mediat. Inflamm. 2016 (2016) 3,481,371.
[56] P.R. Elliott, D. Komander, Regulation of Met1-linked polyubiquitin signalling by the deubiquitinase OTULIN, FEBS J. 283 (2016) 39–53.
[57] S.C. Sun, Deubiquitylation and regulation of the immune response, Nat. Rev. Immunol. 8 (2008) 501–511.
[58] H. Sun, Q. Zhang, Y.Y. Jing, M. Zhang, H.Y. Wang, Z. Cai, et al., USP13 negatively regulates antiviral responses by deubiquitinating STING, Nat. Commun. 8 (2017) 15,534.
[59] B.J. Mathis, Y. Lai, C. Qu, J.S. Janicki, T. Cui, CYLD-mediated signaling and diseases, Curr. Drug Targets 16 (2015) 284–294.
[60] L. Catrysse, L. Vereecke, R. Beyaert, G. van Loo, A20 in inflammation and autoimmunity, Trends Immunol. 35 (2014) 22–31.
[61] B.R. tenOever, The evolution of antiviral defense systems, Cell Host Microbe 19 (2016) 142–149.
[62] A.S. Lauring, J. Frydman, R. Andino, The role of mutational robustness in RNA virus evolution, Nat. Rev. Microbiol. 11 (2013) 327–336.
[63] E.V. Koonin, V.V. Dolja, M. Krupovic, Origins and evolution of viruses of eukaryotes: the ultimate modularity, Virology 479–480 (2015) 2–25.
[64] Y.K. Chan, M.U. Gack, Viral evasion of intracellular DNA and RNA sensing, Nat. Rev. Microbiol. 14 (2016) 360–373.
[65] D.C. Beachboard, S.M. Horner, Innate immune evasion strategies of DNA and RNA viruses, Curr. Opin. Microbiol. 32 (2016) 113–119.
[66] M.K. Isaacson, H.L. Ploegh, Ubiquitination, ubiquitin-like modifiers, and deubiquitination in viral infection, Cell Host Microbe 5 (2009) 559–570.
[67] F. Randow, P.J. Lehner, Viral avoidance and exploitation of the ubiquitin system, Nat. Cell Biol. 11 (2009) 527–534.
[68] Z. Gu, W. Shi, Manipulation of viral infection by deubiquitinating enzymes: new players in host-virus interactions, Future Microbiol. 11 (2016) 1435–1446.
[69] C. Zhang, D. Zhou, Adenoviral vector-based strategies against infectious disease and cancer, Hum. Vaccin. Immunother. 12 (2016) 2064–2074.
[70] A.J. Berk, Fields Virology, in: D.M. Knipe, P.M. Howley (Eds.), Adenoviridae, Chapter 55, 6th edit., 2, Wolters Kluwer/Lippincott Williams & Wilkins Health, Philadelphia, PA 2013, pp. 1704–1731.
[71] J. Weber, Genetic analysis of adenovirus type 2 III. Temperature sensitivity of processing viral proteins, J. Virol. 17 (1976) 462–471.
[72] A. Webster, S. Russell, P. Talbot, W.C. Russell, G.D. Kemp, Characterization of the adenovirus proteinase: substrate specificity, J. Gen. Virol. 70 (1989) 3225–3234.
[73] W.F. Mangel, W.J. McGrath, D.L. Toledo, C.W. Anderson, Viral DNA and a viral peptide can act as cofactors of adenovirus virion proteinase activity, Nature 361 (1993) 274–275.
[74] M.Y. Balakirev, M. Jaquinod, A.L. Haas, J. Chroboczek, Deubiquitinating function of adenovirus proteinase, J. Virol. 76 (2002) 6323–6331.
[75] J. Ding, W.J. McGrath, R.M. Sweet, W.F. Mangel, Crystal structure of the human adenovirus proteinase with its 11 amino acid cofactor, EMBO J. 15 (1996) 1778–1783.
[76] I.G. Kamphuis, K.H. Kalk, M.B. Swarte, J. Drenth, Structure of papain refined at 1.65 a resolution, J. Mol. Biol. 179 (1984) 233–256.
[77] M.L. Baniecki, W.J. McGrath, W.F. Mangel, Regulation of a viral proteinase by a peptide and DNA in one-dimensional space: III. Atomic resolution structure of the nascent form of the adenovirus proteinase, J. Biol. Chem. 288 (2013) 2081–2091.
[78] N.D. Rawlings, A.J. Barrett, R. Finn, Twenty years of the MEROPS database of proteolytic enzymes, their substrates and inhibitors, Nucleic Acids Res. 44 (2016) D343–D350.
[79] S. Gupta, W.F. Mangel, W.J. McGrath, J.L. Perek, D.W. Lee, K. Takamoto, et al., DNA binding provides a molecular strap activating the adenovirus proteinase, Mol. Cell. Proteomics 3 (2004) 950–959.
[80] B. Roizman, R.J. Whitley, An inquiry into the molecular basis of HSV latency and reactivation, Annu. Rev. Microbiol. 67 (2013) 355–374.
[81] H.C. Jha, Y. Pei, E.S. Robertson, Epstein–Barr virus: diseases linked to infection and transformation, Front. Microbiol. 7 (2016) 1602.
[82] R. Sompallae, S. Gastaldello, S. Hildebrand, N. Zinin, G. Hassink, K. Lindsten, et al., Epstein-barr virus encodes three bona fide ubiquitin-specific proteases, J. Virol. 82 (2008) 10,477–10,486.
[83] A. Borodovsky, H. Ovaa, N. Kolli, T. Gan-Erdene, K.D. Wilkinson, H.L. Ploegh, et al., Chemistry-based functional proteomics reveals novel members of the deubiquitinating enzyme family, Chem. Biol. 9 (2002) 1149–1159.
[84] A. Borodovsky, B.M. Kessler, R. Casagrande, H.S. Overkleeft, K.D. Wilkinson, H.L. Ploegh, A novel active site-directed probe specific for deubiquitylating enzymes reveals proteasome association of USP14, EMBO J. 20 (2001) 5187–5196.
[85] L.M. Kattenhorn, G.A. Korbel, B.M. Kessler, E. Spooner, H.L. Ploegh, A deubiquitinating enzyme encoded by HSV-1 belongs to a family of cysteine proteases that is conserved across the family Herpesviridae, Mol. Cell 19 (2005) 547–557.

[86] E.T. Kim, S.E. Oh, Y.O. Lee, W. Gibson, J.H. Ahn, Cleavage specificity of the UL48 deubiquitinating protease activity of human cytomegalovirus and the growth of an active-site mutant virus in cultured cells, J. Virol. 83 (2009) 12,046–12,056.
[87] S.R. Paludan, A.G. Bowie, K.A. Horan, K.A. Fitzgerald, Recognition of herpesviruses by the innate immune system, Nat. Rev. Immunol. 11 (2011) 143–154.
[88] S. Wang, K. Wang, J. Li, C. Zheng, Herpes simplex virus 1 ubiquitin-specific protease UL36 inhibits beta interferon production by deubiquitinating TRAF3, J. Virol. 87 (2013) 11,851–11,860.
[89] R. Ye, C. Su, H. Xu, C. Zheng, Herpes simplex virus 1 ubiquitin-specific protease UL36 abrogates NF-kappaB activation in DNA sensing signal pathway, J. Virol. 91 (2017) e02417-16.
[90] C. Schlieker, G.A. Korbel, L.M. Kattenhorn, H.L. Ploegh, A deubiquitinating activity is conserved in the large tegument protein of the herpesviridae, J. Virol. 79 (2005) 15,582–15,585.
[91] C. Schlieker, W.A. Weihofen, E. Frijns, L.M. Kattenhorn, R. Gaudet, H.L. Ploegh, Structure of a herpesvirus-encoded cysteine protease reveals a unique class of deubiquitinating enzymes, Mol. Cell 25 (2007) 677–687.
[92] A.T. Hilterbrand, D.R. Boutz, E.M. Marcotte, J.W. Upton, Murine cytomegalovirus deubiquitinase regulates viral chemokine levels to control inflammation and pathogenesis, MBio 8 (2017) e01864-16.
[93] M.A. Calderwood, K. Venkatesan, L. Xing, M.R. Chase, A. Vazquez, A.M. Holthaus, et al., Epstein–Barr virus and virus human protein interaction maps, Proc. Natl. Acad. Sci. U. S. A. 104 (2007) 7606–7611.
[94] C.B. Whitehurst, S. Ning, G.L. Bentz, F. Dufour, E. Gershburg, J. Shackelford, et al., The Epstein–Barr virus (EBV) deubiquitinating enzyme BPLF1 reduces EBV ribonucleotide reductase activity, J. Virol. 83 (2009) 4345–4353.
[95] S. Gastaldello, S. Hildebrand, O. Faridani, S. Callegari, M. Palmkvist, C. Di Guglielmo, et al., A deneddylase encoded by Epstein–Barr virus promotes viral DNA replication by regulating the activity of cullin-RING ligases, Nat. Cell Biol. 12 (2010) 351–361.
[96] D.M. Duda, D.C. Scott, M.F. Calabrese, E.S. Zimmerman, N. Zheng, B.A. Schulman, Structural regulation of cullin-RING ubiquitin ligase complexes, Curr. Opin. Struct. Biol. 21 (2011) 257–264.
[97] C.B. Whitehurst, G. Li, S.A. Montgomery, N.D. Montgomery, L. Su, J.S. Pagano, Knockout of Epstein–Barr virus BPLF1 retards B-cell transformation and lymphoma formation in humanized mice, MBio 6 (2015) e01574–15.
[98] C.B. Whitehurst, C. Vaziri, J. Shackelford, J.S. Pagano, Epstein–Barr virus BPLF1 deubiquitinates PCNA and attenuates polymerase eta recruitment to DNA damage sites, J. Virol. 86 (2012) 8097–8106.
[99] S. Saito, T. Murata, T. Kanda, H. Isomura, Y. Narita, A. Sugimoto, et al., Epstein–Barr virus deubiquitinase downregulates TRAF6-mediated NF-kappaB signaling during productive replication, J. Virol. 87 (2013) 4060–4070.
[100] M. van Gent, S.G. Braem, A. de Jong, N. Delagic, J.G. Peeters, I.G. Boer, et al., Epstein–Barr virus large tegument protein BPLF1 contributes to innate immune evasion through interference with toll-like receptor signaling, PLoS Pathog. 10 (2014) e1003960.
[101] J. Wang, A.N. Loveland, L.M. Kattenhorn, H.L. Ploegh, W. Gibson, High-molecular-weight protein (pUL48) of human cytomegalovirus is a competent deubiquitinating protease: mutant viruses altered in its active-site cysteine or histidine are viable, J. Virol. 80 (2006) 6003–6012.
[102] S. Gredmark, C. Schlieker, V. Quesada, E. Spooner, H.L. Ploegh, A functional ubiquitin-specific protease embedded in the large tegument protein (ORF64) of murine gammaherpesvirus 68 is active during the course of infection, J. Virol. 81 (2007) 10,300–10,309.
[103] C.M. Gonzalez, L. Wang, B. Damania, Kaposi's sarcoma-associated herpesvirus encodes a viral deubiquitinase, J. Virol. 83 (2009) 10,224–10,233.
[104] K. Jarosinski, L. Kattenhorn, B. Kaufer, H. Ploegh, N. Osterrieder, A herpesvirus ubiquitin-specific protease is critical for efficient T cell lymphoma formation, Proc. Natl. Acad. Sci. U. S. A. 104 (2007) 20,025–20,030.
[105] K.S. Inn, S.H. Lee, J.Y. Rathbun, L.Y. Wong, Z. Toth, K. Machida, et al., Inhibition of RIG-I-mediated signaling by Kaposi's sarcoma-associated herpesvirus-encoded deubiquitinase ORF64, J. Virol. 85 (2011) 10,899–10,904.
[106] S. Bottcher, C. Maresch, H. Granzow, B.G. Klupp, J.P. Teifke, T.C. Mettenleiter, Mutagenesis of the active-site cysteine in the ubiquitin-specific protease contained in large tegument protein pUL36 of pseudorabies virus impairs viral replication *in vitro* and neuroinvasion *in vivo*, J. Virol. 82 (2008) 6009–6016.
[107] N.J. Huffmaster, P.J. Sollars, A.L. Richards, G.E. Pickard, G.A. Smith, Dynamic ubiquitination drives herpesvirus neuroinvasion, Proc. Natl. Acad. Sci. U. S. A. 112 (2015) 12,818–12,823.
[108] N.S. Zhong, B.J. Zheng, Y.M. Li, Poon, Z.H. Xie, K.H. Chan, et al., Epidemiology and cause of severe acute respiratory syndrome (SARS) in Guangdong, People's Republic of China, in February, 2003, Lancet 362 (2003) 1353–1358.
[109] C. Drosten, S. Gunther, W. Preiser, S. van der Werf, H.R. Brodt, S. Becker, et al., Identification of a novel coronavirus in patients with severe acute respiratory syndrome, N. Engl. J. Med. 348 (2003) 1967–1976.
[110] T.G. Ksiazek, D. Erdman, C.S. Goldsmith, S.R. Zaki, T. Peret, S. Emery, et al., A novel coronavirus associated with severe acute respiratory syndrome, N. Engl. J. Med. 348 (2003) 1953–1966.
[111] J.S. Peiris, S.T. Lai, L.L. Poon, Y. Guan, L.Y. Yam, W. Lim, et al., Coronavirus as a possible cause of severe acute respiratory syndrome, Lancet 361 (2003) 1319–1325.
[112] A.M. Zaki, S. van Boheemen, T.M. Bestebroer, A.D. Osterhaus, R.A. Fouchier, Isolation of a novel coronavirus from a man with pneumonia in Saudi Arabia, N. Engl. J. Med. 367 (2012) 1814–1820.
[113] WHO. Middle east respiratory syndrome coronavirus (MERS-CoV)—Saudi Arabia http://www.who.int/mediacentre/factsheets/mers-cov/en/.
[114] V.S. Raj, E.A. Farag, C.B. Reusken, M.M. Lamers, S.D. Pas, J. Voermans, et al., Isolation of MERS coronavirus from a dromedary camel, Qatar, 2014, Emerg. Infect. Dis. 20 (2014) 1339–1342.
[115] Y. Guan, B.J. Zheng, Y.Q. He, X.L. Liu, Z.X. Zhuang, C.L. Cheung, et al., Isolation and characterization of viruses related to the SARS coronavirus from animals in southern China, Science 302 (2003) 276–278.
[116] L. van der Hoek, K. Pyrc, M.F. Jebbink, W. Vermeulen-Oost, R.J. Berkhout, K.C. Wolthers, et al., Identification of a new human coronavirus, Nat. Med. 10 (2004) 368–373.
[117] D. Hamre, J.J. Procknow, A new virus isolated from the human respiratory tract, Proc. Soc. Exp. Biol. Med. 121 (1966) 190–193.

[118] L. van der Hoek, K. Sure, G. Ihorst, A. Stang, K. Pyrc, M.F. Jebbink, et al., Croup is associated with the novel coronavirus NL63, PLoS Med. 2 (2005) e240.
[119] T.E. Lane, M.P. Hosking, The pathogenesis of murine coronavirus infection of the central nervous system, Crit. Rev. Immunol. 30 (2010) 119–130.
[120] C. Lee, Porcine epidemic diarrhea virus: an emerging and re-emerging epizootic swine virus, Virol. J. 12 (2015) 193.
[121] S. Perlman, J. Netland, Coronaviruses post-SARS: update on replication and pathogenesis, Nat. Rev. Microbiol. 7 (2009) 439–450.
[122] P.A. Rota, M.S. Oberste, S.S. Monroe, W.A. Nix, R. Campagnoli, J.P. Icenogle, et al., Characterization of a novel coronavirus associated with severe acute respiratory syndrome, Science 300 (2003) 1394–1399.
[123] M.A. Marra, S.J. Jones, C.R. Astell, R.A. Holt, A. Brooks-Wilson, Y.S. Butterfield, et al., The genome sequence of the SARS-associated coronavirus, Science 300 (2003) 1399–1404.
[124] Y.J. Ruan, C.L. Wei, A.L. Ee, V.B. Vega, H. Thoreau, S.T. Su, et al., Comparative full-length genome sequence analysis of 14 SARS coronavirus isolates and common mutations associated with putative origins of infection, Lancet 361 (2003) 1779–1785.
[125] E.J. Snijder, P.J. Bredenbeek, J.C. Dobbe, V. Thiel, J. Ziebuhr, L.L. Poon, et al., Unique and conserved features of genome and proteome of SARS-coronavirus, an early split-off from the coronavirus group 2 lineage, J. Mol. Biol. 331 (2003) 991–1004.
[126] V. Thiel, K.A. Ivanov, A. Putics, T. Hertzig, B. Schelle, S. Bayer, et al., Mechanisms and enzymes involved in SARS coronavirus genome expression, J. Gen. Virol. 84 (2003) 2305–2315.
[127] B.H. Harcourt, D. Jukneliene, A. Kanjanahaluethai, J. Bechill, K.M. Severson, C.M. Smith, et al., Identification of severe acute respiratory syndrome coronavirus replicase products and characterization of papain-like protease activity, J. Virol. 78 (2004) 13,600–13,612.
[128] T. Sulea, H.A. Lindner, E.O. Purisima, R. Menard, Deubiquitination, a new function of the severe acute respiratory syndrome coronavirus papain-like protease? J. Virol. 79 (2005) 4550–4551.
[129] N. Barretto, D. Jukneliene, K. Ratia, Z. Chen, A.D. Mesecar, S.C. Baker, The papain-like protease of severe acute respiratory syndrome coronavirus has deubiquitinating activity, J. Virol. 79 (2005) 15,189–15,198.
[130] H.A. Lindner, N. Fotouhi-Ardakani, V. Lytvyn, P. Lachance, T. Sulea, R. Ménard, The papain-like protease from the severe acute respiratory syndrome coronavirus is a deubiquitinating enzyme, J. Virol. 79 (2005) 15,199–15,208.
[131] S.G. Devaraj, N. Wang, Z. Chen, Z. Chen, M. Tseng, N. Barretto, et al., Regulation of IRF-3-dependent innate immunity by the papain-like protease domain of the severe acute respiratory syndrome coronavirus, J. Biol. Chem. 282 (2007) 32,208–32,221.
[132] M. Spiegel, A. Pichlmair, L. Martinez-Sobrido, J. Cros, A. Garcia-Sastre, O. Haller, et al., Inhibition of beta interferon induction by severe acute respiratory syndrome coronavirus suggests a two-step model for activation of interferon regulatory factor 3, J. Virol. 79 (2005) 2079–2086.
[133] M. Frieman, K. Ratia, R.E. Johnston, A.D. Mesecar, R.S. Baric, Severe acute respiratory syndrome coronavirus papain-like protease ubiquitin-like domain and catalytic domain regulate antagonism of IRF3 and NF-kappaB signaling, J. Virol. 83 (2009) 6689–6705.
[134] K. Matthews, A. Schafer, A. Pham, M. Frieman, The SARS coronavirus papain like protease can inhibit IRF3 at a post activation step that requires deubiquitination activity, Virol. J. 11 (2014) 209.
[135] K. Ratia, K.S. Saikatendu, B.D. Santarsiero, N. Barretto, S.C. Baker, R.C. Stevens, et al., Severe acute respiratory syndrome coronavirus papain-like protease: structure of a viral deubiquitinating enzyme, Proc. Natl. Acad. Sci. U. S. A. 103 (2006) 5717–5722.
[136] M. Hu, P. Li, M. Li, W. Li, T. Yao, J.W. Wu, et al., Crystal structure of a UBP-family deubiquitinating enzyme in isolation and in complex with ubiquitin aldehyde, Cell 111 (2002) 1041–1054.
[137] R. Chaudhuri, S. Tang, G. Zhao, H. Lu, D.A. Case, M.E. Johnson, Comparison of SARS and NL63 papain-like protease binding sites and binding site dynamics: inhibitor design implications, J. Mol. Biol. 414 (2011) 272–288.
[138] M.A. Clementz, Z. Chen, B.S. Banach, Y. Wang, L. Sun, K. Ratia, et al., Deubiquitinating and interferon antagonism activities of coronavirus papain-like proteases, J. Virol. 84 (2010) 4619–4629.
[139] M. Bekes, W. Rut, P. Kasperkiewicz, M.P. Mulder, H. Ovaa, M. Drag, et al., SARS hCoV papain-like protease is a unique Lys48 linkage-specific di-distributive deubiquitinating enzyme, Biochem. J. 468 (2015) 215–226.
[140] C.Y. Chou, H.Y. Lai, H.Y. Chen, S.C. Cheng, K.W. Cheng, Y.W. Chou, Structural basis for catalysis and ubiquitin recognition by the severe acute respiratory syndrome coronavirus papain-like protease, Acta Crystallogr. D Biol. Crystallogr. 70 (2014) 572–581.
[141] C.M. Daczkowski, J.V. Dzimianski, J.R. Clasman, O. Goodwin, A.D. Mesecar, S.D. Pegan, Structural insights into the interaction of coronavirus papain-like proteases and interferon-stimulated gene product 15 from different species, J. Mol. Biol. 429 (2017) 1661–1683.
[142] M. Bekes, G.J. van der Heden van Noort, R. Ekkebus, H. Ovaa, T.T. Huang, C.D. Lima, Recognition of Lys48-linked di-ubiquitin and deubiquitinating activities of the SARS coronavirus papain-like protease, Mol. Cell 62 (2016) 572–585.
[143] Z.M. Eletr, K.D. Wilkinson, Regulation of proteolysis by human deubiquitinating enzymes, Biochim. Biophys. Acta 2014 (1843) 114–128.
[144] K. Ratia, A. Kilianski, Y.M. Baez-Santos, S.C. Baker, A. Mesecar, Structural basis for the ubiquitin-linkage specificity and deISGylating activity of SARS-CoV papain-like protease, PLoS Pathog. 10 (2014) e1004113.
[145] M. Drag, J. Mikolajczyk, M. Bekes, F.E. Reyes-Turcu, J.A. Ellman, K.D. Wilkinson, et al., Positional-scanning fluorigenic substrate libraries reveal unexpected specificity determinants of DUBs (deubiquitinating enzymes), Biochem. J. 415 (2008) 367–375.
[146] Y.S. Han, G.G. Chang, C.G. Juo, H.J. Lee, S.H. Yeh, J.T. Hsu, et al., Papain-like protease 2 (PLP2) from severe acute respiratory syndrome coronavirus (SARS-CoV): expression, purification, characterization, and inhibition, Biochemistry 44 (2005) 10,349–10,359.
[147] C.Y. Chou, C.H. Chien, Y.S. Han, M.T. Prebanda, H.P. Hsieh, B. Turk, et al., Thiopurine analogues inhibit papain-like protease of severe acute respiratory syndrome coronavirus, Biochem. Pharmacol. 75 (2008) 1601–1609.
[148] K. Ratia, S. Pegan, J. Takayama, K. Sleeman, M. Coughlin, S. Baliji, et al., A noncovalent class of papain-like protease/deubiquitinase inhibitors blocks SARS virus replication, Proc. Natl. Acad. Sci. U. S. A. 105 (2008) 16,119–16,124.

[149] X. Chen, C.Y. Chou, G.G. Chang, Thiopurine analogue inhibitors of severe acute respiratory syndrome-coronavirus papain-like protease, a deubiquitinating and deISGylating enzyme, Antivir. Chem. Chemother. 19 (2009) 151–156.
[150] A.K. Ghosh, J. Takayama, Y. Aubin, K. Ratia, R. Chaudhuri, Y. Baez, et al., Structure-based design, synthesis, and biological evaluation of a series of novel and reversible inhibitors for the severe acute respiratory syndrome-coronavirus papain-like protease, J. Med. Chem. 52 (2009) 5228–5240.
[151] A.K. Ghosh, J. Takayama, K.V. Rao, K. Ratia, R. Chaudhuri, D.C. Mulhearn, et al., Severe acute respiratory syndrome coronavirus papain-like novel protease inhibitors: design, synthesis, protein-ligand X-ray structure and biological evaluation, J. Med. Chem. 53 (2010) 4968–4979.
[152] H. Lee, S. Cao, K.E. Hevener, L. Truong, J.L. Gatuz, K. Patel, et al., Synergistic inhibitor binding to the papain-like protease of human SARS coronavirus: mechanistic and inhibitor design implications, ChemMedChem 8 (2013) 1361–1372.
[153] Y.M. Baez-Santos, S.J. Barraza, M.W. Wilson, M.P. Agius, A.M. Mielech, N.M. Davis, et al., X-ray structural and biological evaluation of a series of potent and highly selective inhibitors of human coronavirus papain-like proteases, J. Med. Chem. 57 (2014) 2393–2412.
[154] Y.M. Baez-Santos, S.E. St John, A.D. Mesecar, The SARS-coronavirus papain-like protease: structure, function and inhibition by designed antiviral compounds, Antivir. Res. 115 (2015) 21–38.
[155] S. van Boheemen, M. de Graaf, C. Lauber, T.M. Bestebroer, V.S. Raj, A.M. Zaki, et al., Genomic characterization of a newly discovered coronavirus associated with acute respiratory distress syndrome in humans, mBio 3 (2012) e00473-12.
[156] A. Kilianski, A.M. Mielech, X. Deng, S.C. Baker, Assessing activity and inhibition of Middle East respiratory syndrome coronavirus papain-like and 3C-like proteases using luciferase-based biosensors, J. Virol. 87 (2013) 11,955–11,962.
[157] X. Yang, X. Chen, G. Bian, J. Tu, Y. Xing, Y. Wang, et al., Proteolytic processing, deubiquitinase and interferon antagonist activities of Middle East respiratory syndrome coronavirus papain-like protease, J. Gen. Virol. 95 (2014) 614–626.
[158] Y.M. Baez-Santos, A.M. Mielech, X. Deng, S. Baker, A.D. Mesecar, Catalytic function and substrate specificity of the papain-like protease domain of nsp3 from the Middle East respiratory syndrome coronavirus, J. Virol. 88 (2014) 12,511–12,527.
[159] J. Lei, J.R. Mesters, C. Drosten, S. Anemuller, Q. Ma, R. Hilgenfeld, Crystal structure of the papain-like protease of MERS coronavirus reveals unusual, potentially druggable active-site features, Antivir. Res. 109 (2014) 72–82.
[160] M.H. Lin, S.J. Chuang, C.C. Chen, S.C. Cheng, K.W. Cheng, C.H. Lin, et al., Structural and functional characterization of MERS coronavirus papain-like protease, J. Biomed. Sci. 21 (2014) 54.
[161] J. Lei, R. Hilgenfeld, Structural and mutational analysis of the interaction between the Middle-East respiratory syndrome coronavirus (MERS-CoV) papain-like protease and human ubiquitin, Virol. Sin. 31 (2016) 288–299.
[162] B.A. Bailey-Elkin, R.C. Knaap, G.G. Johnson, T.J. Dalebout, D.K. Ninaber, P.B. van Kasteren, et al., Crystal structure of the Middle East respiratory syndrome coronavirus (MERS-CoV) papain-like protease bound to ubiquitin facilitates targeted disruption of deubiquitinating activity to demonstrate its role in innate immune suppression, J. Biol. Chem. 289 (2014) 34,667–34,682.
[163] A.M. Mielech, A. Kilianski, Y.M. Baez-Santos, A.D. Mesecar, S.C. Baker, MERS-CoV papain-like protease has deISGylating and deubiquitinating activities, Virology 450–451 (2014) 64–70.
[164] H. Lee, H. Lei, B.D. Santarsiero, J.L. Gatuz, S. Cao, A.J. Rice, et al., Inhibitor recognition specificity of MERS-CoV papain-like protease may differ from that of SARS-CoV, ACS Chem. Biol. 10 (2015) 1456–1465.
[165] R. Hilgenfeld, From SARS to MERS: crystallographic studies on coronaviral proteases enable antiviral drug design, FEBS J. 281 (2014) 4085–4096.
[166] J.R. Clasman, Y.M. Baez-Santos, R.C. Mettelman, A. O'Brien, S.C. Baker, A.D. Mesecar, X-ray structure and enzymatic activity profile of a core papain-like protease of MERS coronavirus with utility for structure-based drug design, Sci. Rep. 7 (2017) 40,292.
[167] W. Zhang, K.P. Wu, M.A. Sartori, H.B. Kamadurai, A. Ordureau, C. Jiang, et al., System-wide modulation of HECT E3 ligases with selective ubiquitin variant probes, Mol. Cell 62 (2016) 121–136.
[168] M. Gorelik, S. Orlicky, M.A. Sartori, X. Tang, E. Marcon, I. Kurinov, et al., Inhibition of SCF ubiquitin ligases by engineered ubiquitin variants that target the Cul1 binding site on the Skp1-F-box interface, Proc. Natl. Acad. Sci. U. S. A. 113 (2016) 3527–3532.
[169] A. Ernst, G. Avvakumov, J. Tong, Y. Fan, Y. Zhao, P. Alberts, et al., A strategy for modulation of enzymes in the ubiquitin system, Science 339 (2013) 590–595.
[170] N. Manczyk, B.P. Yates, G. Veggiani, A. Ernst, F. Sicheri, S.S. Sidhu, Structural and functional characterization of a ubiquitin variant engineered for tight and specific binding to an alpha-helical ubiquitin interacting motif, Protein Sci. 26 (2017) 1060–1069.
[171] W. Zhang, B.A. Bailey-Elkin, R.C.M. Knaap, B. Khare, T.J. Dalebout, G.G. Johnson, et al., Potent and selective inhibition of pathogenic viruses by engineered ubiquitin variants, PLoS Pathog. 13 (2017) e1006372.
[172] Z. Chen, Y. Wang, K. Ratia, A.D. Mesecar, K.D. Wilkinson, S.C. Baker, Proteolytic processing and deubiquitinating activity of papain-like proteases of human coronavirus NL63, J. Virol. 81 (2007) 6007–6018.
[173] B. Nicholson, C.A. Leach, S.J. Goldenberg, D.M. Francis, M.P. Kodrasov, X. Tian, et al., Characterization of ubiquitin and ubiquitin-like-protein isopeptidase activities, Protein Sci. 17 (2008) 1035–1043.
[174] L. Sun, Y. Xing, X. Chen, Y. Zheng, Y. Yang, D.B. Nichols, et al., Coronavirus papain-like proteases negatively regulate antiviral innate immune response through disruption of STING-mediated signaling, PLoS One 7 (2012) e30802.
[175] H.J. Lee, C.K. Shieh, A.E. Gorbalenya, E.V. Koonin, N. La Monica, J. Tuler, et al., The complete sequence (22 kilobases) of murine coronavirus gene 1 encoding the putative proteases and RNA polymerase, Virology 180 (1991) 567–582.
[176] A. Kanjanahaluethai, S.C. Baker, Identification of mouse hepatitis virus papain-like proteinase 2 activity, J. Virol. 74 (2000) 7911–7921.
[177] Y. Chen, S.N. Savinov, A.M. Mielech, T. Cao, S.C. Baker, A.D. Mesecar, X-ray structural and functional studies of the three tandemly linked domains of non-structural protein 3 (nsp3) from murine hepatitis virus reveal conserved functions, J. Biol. Chem. 290 (2015) 25,293–25,306.
[178] G. Wang, G. Chen, D. Zheng, G. Cheng, H. Tang, PLP2 of mouse hepatitis virus A59 (MHV-A59) targets TBK1 to

negatively regulate cellular type I interferon signaling pathway, PLoS One 6 (2011) e17192.
[179] D. Zheng, G. Chen, B. Guo, G. Cheng, H. Tang, PLP2, a potent deubiquitinase from murine hepatitis virus, strongly inhibits cellular type I interferon production, Cell Res. 18 (2008) 1105–1113.
[180] A.M. Mielech, X. Deng, Y. Chen, E. Kindler, D.L. Wheeler, A.D. Mesecar, et al., Murine coronavirus ubiquitin-like domain is important for papain-like protease stability and viral pathogenesis, J. Virol. 89 (2015) 4907–4917.
[181] A. Putics, A.E. Gorbalenya, J. Ziebuhr, Identification of protease and ADP-ribose 1″-monophosphatase activities associated with transmissible gastroenteritis virus non-structural protein 3, J. Gen. Virol. 87 (2006) 651–656.
[182] J.A. Wojdyla, I. Manolaridis, P.B. van Kasteren, M. Kikkert, E.J. Snijder, A.E. Gorbalenya, et al., Papain-like protease 1 from transmissible gastroenteritis virus: crystal structure and enzymatic activity toward viral and cellular substrates, J. Virol. 84 (2010) 10,063–10,073.
[183] Y. Xing, J. Chen, J. Tu, B. Zhang, X. Chen, H. Shi, et al., The papain-like protease of porcine epidemic diarrhea virus negatively regulates type I interferon pathway by acting as a viral deubiquitinase, J. Gen. Virol. 94 (2013) 1554–1567.
[184] D.X. Liu, K.W. Tibbles, D. Cavanagh, T.D. Brown, I. Brierley, Identification, expression, and processing of an 87-kDa polypeptide encoded by ORF 1a of the coronavirus infectious bronchitis virus, Virology 208 (1995) 48–57.
[185] K.P. Lim, D.X. Liu, Characterization of the two overlapping papain-like proteinase domains encoded in gene 1 of the coronavirus infectious bronchitis virus and determination of the C-terminal cleavage site of an 87-kDa protein, Virology 245 (1998) 303–312.
[186] K.P. Lim, D.X. Liu, Characterisation of a papain-like proteinase domain encoded by ORF1a of the coronavirus IBV and determination of the C-terminal cleavage site of an 87 kDa protein, Adv. Exp. Med. Biol. 440 (1998) 173–184.
[187] K.P. Lim, L.F. Ng, D.X. Liu, Identification of a novel cleavage activity of the first papain-like proteinase domain encoded by open reading frame 1a of the coronavirus avian infectious bronchitis virus and characterization of the cleavage products, J. Virol. 74 (2000) 1674–1685.
[188] L. Kong, N. Shaw, L. Yan, Z. Lou, Z. Rao, Structural view and substrate specificity of papain-like protease from avian infectious bronchitis virus, J. Biol. Chem. 290 (2015) 7160–7168.
[189] L. Yu, X. Zhang, T. Wu, Y. Wang, J. Meng, Q. Liu, et al., The papain-like protease of avian infectious bronchitis virus has deubiquitinating activity, Arch. Virol. 162 (2017) 1943–1950.
[190] C. Lauber, J.J. Goeman, C. Parquet Mdel, P.T. Nga, E.J. Snijder, K. Morita, et al., The footprint of genome architecture in the largest genome expansion in RNA viruses, PLoS Pathog. 9 (2013) e1003500.
[191] E.J. Snijder, M. Kikkert, Y. Fang, Arterivirus molecular biology and pathogenesis, J. Gen. Virol. 94 (2013) 2141–2163.
[192] E.J. Neumann, J.B. Kliebenstein, C.D. Johnson, J.W. Mabry, E.J. Bush, A.H. Seitzinger, et al., Assessment of the economic impact of porcine reproductive and respiratory syndrome on swine production in the United States, J. Am. Vet. Med. Assoc. 227 (2005) 385–392.
[193] D.J. Holtkamp, J.B. Kliebenstein, E.J. Neumann, J.J. Zimmerman, H.F. Rotto, T.K. Yoder, et al., Porcine reproductive and respiratory syndrome (PRRS) is the most economically important disease of swine in North America, Europe and Asia, costing producers in North America more than $600 million annually, J. Swine Health Prod. 21 (2013) 72–84.
[194] H.A. Vatter, H. Di, E.F. Donaldson, G.U. Radu, T.R. Maines, M.A. Brinton, Functional analyses of the three simian hemorrhagic fever virus nonstructural protein 1 papain-like proteases, J. Virol. 88 (2014) 9129–9140.
[195] E.J. Snijder, A.L. Wassenaar, W.J. Spaan, A.E. Gorbalenya, The arterivirus Nsp2 protease. An unusual cysteine protease with primary structure similarities to both papain-like and chymotrypsin-like proteases, J. Biol. Chem. 270 (1995) 16,671–16,676.
[196] P.B. van Kasteren, C. Beugeling, D.K. Ninaber, N. Frias-Staheli, S. van Boheemen, A. Garcia-Sastre, et al., Arterivirus and nairovirus ovarian tumor domain-containing deubiquitinases target activated RIG-I to control innate immune signaling, J. Virol. 86 (2012) 773–785.
[197] K.S. Makarova, L. Aravind, E.V. Koonin, A novel superfamily of predicted cysteine proteases from eukaryotes, viruses and *Chlamydia pneumoniae*, Trends Biochem. Sci. 25 (2000) 50–52.
[198] N. Frias-Staheli, N.V. Giannakopoulos, M. Kikkert, S.L. Taylor, A. Bridgen, J. Paragas, et al., Ovarian tumor domain-containing viral proteases evade ubiquitin- and ISG15-dependent innate immune responses, Cell Host Microbe 2 (2007) 404–416.
[199] P.B. van Kasteren, B.A. Bailey-Elkin, T.W. James, D.K. Ninaber, C. Beugeling, M. Khajehpour, et al., Deubiquitinase function of arterivirus papain-like protease 2 suppresses the innate immune response in infected host cells, Proc. Natl. Acad. Sci. U. S. A. 110 (2013) E838–E847.
[200] B.A. Bailey-Elkin, P.B. van Kasteren, E.J. Snijder, M. Kikkert, B.L. Mark, Viral OTU deubiquitinases: a structural and functional comparison, PLoS Pathog. 10 (2014) e1003894.
[201] P.B. van Kasteren, R.C. Knaap, P. van den Elzen, E.J. Snijder, U.B. Balasuriya, E. van den Born, et al., *In vivo* assessment of equine arteritis virus vaccine improvement by disabling the deubiquitinase activity of papain-like protease 2, Vet. Microbiol. 178 (2015) 132–137.
[202] J. Han, M.S. Rutherford, K.S. Faaberg, The porcine reproductive and respiratory syndrome virus nsp2 cysteine protease domain possesses both *trans*- and *cis*-cleavage activities, J. Virol. 83 (2009) 9449–9463.
[203] J. Han, M.S. Rutherford, K.S. Faaberg, Proteolytic products of the porcine reproductive and respiratory syndrome virus nsp2 replicase protein, J. Virol. 84 (2010) 10,102–10,112.
[204] Y. Fang, E.E. Treffers, Y. Li, A. Tas, Z. Sun, Y. van der Meer, et al., Efficient −2 frameshifting by mammalian ribosomes to synthesize an additional arterivirus protein, Proc. Natl. Acad. Sci. U. S. A. 109 (2012) E2920–E2928.
[205] Y. Li, E.E. Treffers, S. Napthine, A. Tas, L. Zhu, Z. Sun, et al., Transactivation of programmed ribosomal frameshifting by a viral protein, Proc. Natl. Acad. Sci. U. S. A. 111 (2014) E2172–E2181.
[206] M.A. Kappes, C.L. Miller, K.S. Faaberg, Highly divergent strains of porcine reproductive and respiratory syndrome virus incorporate multiple isoforms of nonstructural protein 2 into virions, J. Virol. 87 (2013) 13,456–13,465.
[207] Z. Sun, Y. Li, R. Ransburgh, E.J. Snijder, Y. Fang, Nonstructural protein 2 of porcine reproductive and respiratory syndrome virus inhibits the antiviral function of interferon-stimulated gene 15, J. Virol. 86 (2012) 3839–3850.
[208] Z. Sun, Z. Chen, S.R. Lawson, Y. Fang, The cysteine protease domain of porcine reproductive and respiratory syndrome virus nonstructural protein 2 possesses

deubiquitinating and interferon antagonism functions, J. Virol. 84 (2010) 7832–7846.
[209] M.K. Deaton, A. Spear, K.S. Faaberg, S.D. Pegan, The vOTU domain of highly-pathogenic porcine reproductive and respiratory syndrome virus displays a differential substrate preference, Virology 454–455 (2014) 247–253.
[210] D.A. Bente, N.L. Forrester, D.M. Watts, A.J. McAuley, C.A. Whitehouse, M. Bray, Crimean-Congo hemorrhagic fever: history, epidemiology, pathogenesis, clinical syndrome and genetic diversity, Antivir. Res. 100 (2013) 159–189.
[211] J. Treib, G. Dobler, A. Haass, W. von Blohn, M. Strittmatter, G. Pindur, et al., Thunderclap headache caused by Erve virus? Neurology 50 (1998) 509–511.
[212] R. Woessner, M.T. Grauer, J. Langenbach, G. Dobler, J. Kroeger, H.G. Mielke, et al., The Erve virus: possible mode of transmission and reservoir, Infection 28 (2000) 164–166.
[213] E. Kinsella, S.G. Martin, A. Grolla, M. Czub, H. Feldmann, R. Flick, Sequence determination of the Crimean-Congo hemorrhagic fever virus L segment, Virology 321 (2004) 23–28.
[214] J.E. Honig, J.C. Osborne, S.T. Nichol, Crimean-Congo hemorrhagic fever virus genome L RNA segment and encoded protein, Virology 321 (2004) 29–35.
[215] P.C. Evans, H. Ovaa, M. Hamon, P.J. Kilshaw, S. Hamm, S. Bauer, et al., Zinc-finger protein A20, a regulator of inflammation and cell survival, has de-ubiquitinating activity, Biochem. J. 378 (2004) 727–734.
[216] D.L. Boone, E.E. Turer, E.G. Lee, R.C. Ahmad, M.T. Wheeler, C. Tsui, et al., The ubiquitin-modifying enzyme A20 is required for termination of toll-like receptor responses, Nat. Immunol. 5 (2004) 1052–1060.
[217] T.W. James, N. Frias-Staheli, J.P. Bacik, J.M. Levingston Macleod, M. Khajehpour, A. Garcia-Sastre, et al., Structural basis for the removal of ubiquitin and interferon-stimulated gene 15 by a viral ovarian tumor domain-containing protease, Proc. Natl. Acad. Sci. U. S. A. 108 (2011) 2222–2227.
[218] M. Akutsu, Y. Ye, S. Virdee, J.W. Chin, D. Komander, Molecular basis for ubiquitin and ISG15 cross-reactivity in viral ovarian tumor domains, Proc. Natl. Acad. Sci. U. S. A. 108 (2011) 2228–2233.
[219] G.C. Capodagli, M.A. McKercher, E.A. Baker, E.M. Masters, J.S. Brunzelle, S.D. Pegan, Structural analysis of a viral ovarian tumor domain protease from the Crimean-Congo hemorrhagic fever virus in complex with covalently bonded ubiquitin, J. Virol. 85 (2011) 3621–3630.
[220] T.E. Messick, N.S. Russell, A.J. Iwata, K.L. Sarachan, R. Shiekhattar, J.R. Shanks, et al., Structural basis for ubiquitin recognition by the Otu1 ovarian tumor domain protein, J. Biol. Chem. 283 (2008) 11,038–11,049.
[221] G.C. Capodagli, M.K. Deaton, E.A. Baker, R.J. Lumpkin, S.D. Pegan, Diversity of ubiquitin and ISG15 specificity among nairoviruses' viral ovarian tumor domain proteases, J. Virol. 87 (2013) 3815–3827.
[222] E. Bergeron, M. Zivcec, A.K. Chakrabarti, S.T. Nichol, C.G. Albarino, C.F. Spiropoulou, Recovery of recombinant Crimean Congo hemorrhagic fever virus reveals a function for non-structural glycoproteins cleavage by Furin, PLoS Pathog. 11 (2015) e1004879.
[223] S. Bakshi, B. Holzer, A. Bridgen, G. McMullan, D.G. Quinn, M.D. Baron, Dugbe virus ovarian tumour domain interferes with ubiquitin/ISG15-regulated innate immune cell signalling, J. Gen. Virol. 94 (2013) 298–307.
[224] M.K. Deaton, J.V. Dzimianski, C.M. Daczkowski, G.K. Whitney, N.J. Mank, M.M. Parham, et al., biochemical and structural insights into the preference of nairoviral deISGylases for interferon-stimulated gene product 15 originating from certain species, J. Virol. 90 (2016) 8314–8327.
[225] B. Holzer, S. Bakshi, A. Bridgen, M.D. Baron, Inhibition of interferon induction and action by the nairovirus Nairobi sheep disease virus/Ganjam virus, PLoS One 6 (2011) e28594.
[226] P. Shang, S. Misra, B. Hause, Y. Fang, A naturally occurring recombinant enterovirus expresses a torovirus deubiquitinase, J. Virol. (2017) http://dx.doi.org/10.1128/JVI.00450-17.
[227] J.N. Burroughs, D.V. Sangar, B.E. Clarke, D.J. Rowlands, A. Billiau, D. Collen, Multiple proteases in foot-and-mouth disease virus replication, J. Virol. 50 (1984) 878–883.
[228] K. Strebel, E. Beck, A second protease of foot-and-mouth disease virus, J. Virol. 58 (1986) 893–899.
[229] R. Kirchweger, E. Ziegler, B.J. Lamphear, D. Waters, H.D. Liebig, W. Sommergruber, et al., Foot-and-mouth disease virus leader proteinase: purification of the Lb form and determination of its cleavage site on eIF-4 gamma, J. Virol. 68 (1994) 5677–5684.
[230] M.E. Piccone, E. Rieder, P.W. Mason, M.J. Grubman, The foot-and-mouth disease virus leader proteinase gene is not required for viral replication, J. Virol. 69 (1995) 5376–5382.
[231] T. de Los Santos, S. de Avila Botton, R. Weiblen, M.J. Grubman, The leader proteinase of foot-and-mouth disease virus inhibits the induction of beta interferon mRNA and blocks the host innate immune response, J. Virol. 80 (2006) 1906–1914.
[232] J. Chinsangaram, M. Koster, M.J. Grubman, Inhibition of L-deleted foot-and-mouth disease virus replication by alpha/beta interferon involves double-stranded RNA-dependent protein kinase, J. Virol. 75 (2001) 5498–5503.
[233] J. Chinsangaram, M.E. Piccone, M.J. Grubman, Ability of foot-and-mouth disease virus to form plaques in cell culture is associated with suppression of alpha/beta interferon, J. Virol. 73 (1999) 9891–9898.
[234] T. de Los Santos, F. Diaz-San Segundo, M.J. Grubman, Degradation of nuclear factor kappa B during foot-and-mouth disease virus infection, J. Virol. 81 (2007) 12,803–12,815.
[235] T. de Los Santos, F.D. Segundo, J. Zhu, M. Koster, C.C. Dias, M.J. Grubman, A conserved domain in the leader proteinase of foot-and-mouth disease virus is required for proper subcellular localization and function, J. Virol. 83 (2009) 1800–1810.
[236] A.E. Gorbalenya, E.V. Koonin, M.M. Lai, Putative papain-related thiol proteases of positive-strand RNA viruses. Identification of rubi- and aphthovirus proteases and delineation of a novel conserved domain associated with proteases of rubi-, alpha- and coronaviruses, FEBS Lett. 288 (1991) 201–205.
[237] A. Guarne, J. Tormo, R. Kirchweger, D. Pfistermueller, I. Fita, T. Skern, Structure of the foot-and-mouth disease virus leader protease: a papain-like fold adapted for self-processing and eIF4G recognition, EMBO J. 17 (1998) 7469–7479.
[238] A.E. Gorbalenya, E.V. Koonin, Endonuclease (R) subunits of type-I and type-III restriction-modification enzymes contain a helicase-like domain, FEBS Lett. 291 (1991) 277–281.
[239] R. Cencic, C. Mayer, M.A. Juliano, L. Juliano, R. Konrat, G. Kontaxis, et al., Investigating the substrate specificity and oligomerisation of the leader protease of foot and mouth

disease virus using NMR, J. Mol. Biol. 373 (2007) 1071–1087.
[240] D. Wang, L. Fang, P. Li, L. Sun, J. Fan, Q. Zhang, et al., The leader proteinase of foot-and-mouth disease virus negatively regulates the type I interferon pathway by acting as a viral deubiquitinase, J. Virol. 85 (2011) 3758–3766.
[241] J.A. Santos, I.E. Gouvea, W.A. Judice, M.A. Izidoro, F.M. Alves, R.L. Melo, et al., Hydrolytic properties and substrate specificity of the foot-and-mouth disease leader protease, Biochemistry 48 (2009) 7948–7958.
[242] J.A. Nogueira Santos, D.M. Assis, I.E. Gouvea, W.A. Judice, M.A. Izidoro, M.A. Juliano, et al., Foot and mouth disease leader protease (Lbpro): investigation of prime side specificity allows the synthesis of a potent inhibitor, Biochimie 94 (2012) 711–718.
[243] J. Steinberger, I. Grishkovskaya, R. Cencic, L. Juliano, M.A. Juliano, T. Skern, Foot-and-mouth disease virus leader proteinase: structural insights into the mechanism of intermolecular cleavage, Virology 468–470 (2014) 397–408.
[244] M.D. Morch, J.C. Boyer, A.L. Haenni, Overlapping open reading frames revealed by complete nucleotide sequencing of turnip yellow mosaic virus genomic RNA, Nucleic Acids Res. 16 (1988) 6157–6173.
[245] K.L. Bransom, J.J. Weiland, T.W. Dreher, Proteolytic maturation of the 206-kDa nonstructural protein encoded by turnip yellow mosaic virus RNA, Virology 184 (1991) 351–358.
[246] K.L. Bransom, T.W. Dreher, Identification of the essential cysteine and histidine residues of the turnip yellow mosaic virus protease, Virology 198 (1994) 148–154.
[247] M.N. Rozanov, G. Drugeon, A.L. Haenni, Papain-like proteinase of turnip yellow mosaic virus: a prototype of a new viral proteinase group, Arch. Virol. 140 (1995) 273–288.
[248] A. Jakubiec, G. Drugeon, L. Camborde, I. Jupin, Proteolytic processing of turnip yellow mosaic virus replication proteins and functional impact on infectivity, J. Virol. 81 (2007) 11,402–11,412.
[249] L. Camborde, S. Planchais, V. Tournier, A. Jakubiec, G. Drugeon, E. Lacassagne, et al., The ubiquitin-proteasome system regulates the accumulation of turnip yellow mosaic virus RNA-dependent RNA polymerase during viral infection, Plant Cell 22 (2010) 3142–3152.
[250] M. Chenon, L. Camborde, S. Cheminant, I. Jupin, A viral deubiquitylating enzyme targets viral RNA-dependent RNA polymerase and affects viral infectivity, EMBO J. 31 (2012) 741–753.
[251] C. Lombardi, M. Ayach, L. Beaurepaire, M. Chenon, J. Andreani, R. Guerois, et al., A compact viral processing proteinase/ubiquitin hydrolase from the OTU family, PLoS Pathog. 9 (2013) e1003560.
[252] A. Ordureau, C. Munch, J.W. Harper, Quantifying ubiquitin signaling, Mol. Cell 58 (2015) 660–676.
[253] D. Flierman, G.J. van der Heden van Noort, R. Ekkebus, P.P. Geurink, T.E. Mevissen, M.K. Hospenthal, et al., Non-hydrolyzable diubiquitin probes reveal linkage-specific reactivity of deubiquitylating enzymes mediated by S2 pockets, Cell Chem. Biol. 23 (2016) 472–482.
[254] M.P. Mulder, F. El Oualid, J. ter Beek, H. Ovaa, A native chemical ligation handle that enables the synthesis of advanced activity-based probes: diubiquitin as a case study, Chembiochem 15 (2014) 946–949.
[255] J.N. Pruneda, C.H. Durkin, P.P. Geurink, H. Ovaa, B. Santhanam, D.W. Holden, et al., The molecular basis for ubiquitin and ubiquitin-like specificities in bacterial effector proteases, Mol. Cell 63 (2016) 261–276.
[256] X. Chen, X. Yang, Y. Zheng, Y. Yang, Y. Xing, Z. Chen, SARS coronavirus papain-like protease inhibits the type I interferon signaling pathway through interaction with the STING–TRAF3–TBK1 complex, Protein Cell 5 (2014) 369–381.
[257] L.L.C. Schrodinger, The PyMOL Molecular Graphics System, Version 1.8, 2015.
[258] P. Brown, W. Pullan, Y. Yang, Y. Zhou, Fast and accurate non-sequential protein structure alignment using a new asymmetric linear sum assignment heuristic, Bioinformatics 32 (2016) 370–377.
[259] P.E. Pellett, B. Roizman, Fields Virology, in: D.M. Knipe, P.M. Howley (Eds.), Herpesviridae, Chapter 59, 6th edit., 2, Wolters Kluwer/Lippincott Williams & Wilkins Health, Philadelphia, PA 2013, pp. 1802–1822.
[260] V.R. Racaniello, Fields Virology, in: D.M. Knipe, P.M. Howley (Eds.), Picornaviridae: The viruses and their replication, Chapter 16, 6th edit., 1, Wolters Kluwer/Lippincott Williams & Wilkins Health, Philadelphia, PA 2013, pp. 453–489.